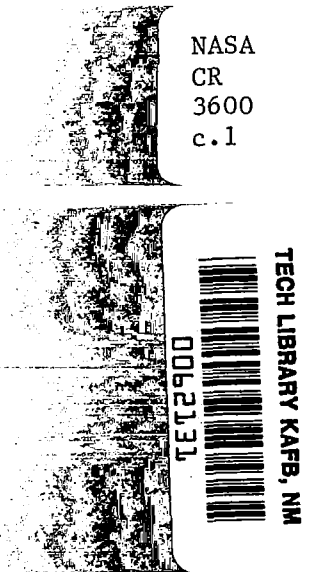

NASA Contractor Report 3600

Rotorcraft Blade Mode Damping Identification From Random Responses Using a Recursive Maximum Likelihood Algorithm

John A. Molusis

SEPTEMBER 1982

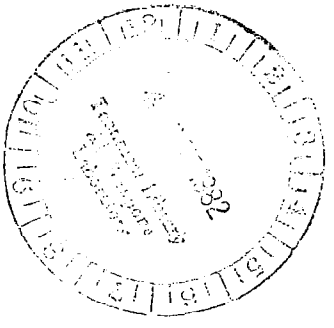

NASA

NASA Contractor Report 3600

Rotorcraft Blade Mode Damping Identification From Random Responses Using a Recursive Maximum Likelihood Algorithm

John A. Molusis
Applied Research Consultant
Ashford, Connecticut

Prepared for NASA
Langley Research Center and
Structures Laboratory, AVRADCOM
Research and Technology Laboratories

NASA
National Aeronautics
and Space Administration

Scientific and Technical
Information Branch

1982

CONTENTS

SUMMARY

An on-line technique is presented for the identification of rotor blade modal damping and frequency from rotorcraft random response test data. The identification technique is based upon a recursive maximum likelihood (RML) algorithm, which is demonstrated to have excellent convergence characteristics in the presence of random measurement noise and random excitation. The RML technique requires virtually no user interaction, provides accurate confidence bands on the parameter estimates, and can be used for continuous monitoring of modal damping and frequency during wind tunnel or flight testing.

Results are presented from simulation random response data which quantify the identified parameter convergence behavior for various levels of random excitation. The data length required for acceptable parameter accuracy is shown to depend upon the amplitude of random response and the modal damping level. Random response amplitudes of 1.25 degrees to .05 degrees are investigated. The RML technique was applied to hingeless rotor test data from the NASA Langley Research Center Helicopter Hover Facility. The inplane lag regressing mode damping was correctly identified at different rotor speeds. The identification from the test data agreed with the simulation results and with other available estimates of frequency and damping.

INTRODUCTION

The determination of rotor blade modal damping for lightly damped rotors during wind tunnel or flight testing is an important safety requirement. Analytic methods to predict stability are often employed before testing, however the accuracy of analytic methods are not always reliable, particularly for new rotor designs or configuration modifications. Estimation of rotor blade mode damping from test data is thus required during wind tunnel testing where the possibility of low damping levels may occur. Current methods for estimation of modal damping from test data are based upon use of the Fast Fourier Transform (FFT). This technique is often referred to as the moving block FFT method. This method has been applied to rotor data obtained either from an initial condition decay response obtained after removal of a forced excitation, or from random response data (ref. 1, ref. 2 and ref. 3). The random response data is first transformed to an initial condition decay response by calculating an ensemble average of segments of the random response time history. Application of the moving block FFT approach is then performed. This technique has been referred to as the moving-block/randomdec method (ref. 1).

During wind tunnel testing, it would be desirable if damping and frequency could be computed without the use of a forced input excitation and be computed in real time along with confidence bands. Although the FFT technique has received widespread acceptance by the rotorcraft community, practical usage of this technique requires considerable user interaction and is not a real time method. Estimation of damping and frequency requires several minutes and continued user

interaction. In addition, wind tunnel applications are usually done with a forced input excitation to obtain the decay response time history.

The RML technique presented in this report requires virtually no user interaction, and provides on-line continuous estimates of damping and frequency from random response data. In addition, accurate confidence bands ($\pm$ 1σ bands) are also recursively computed which indicate the required data length for accurate parameter estimation. The technique can be used on very small amplitude random response data which often is the case in wind tunnel tests. During wind tunnel testing it is common to have data continuously generated while steady trim conditions are achieved, and this data is suitable for parameter identification. Thus, the identification procedure need not interfere with other wind tunnel test objectives. Although the RML technique presented is developed for any number of modes, including closely spaced or overlapping modes, the simulation and test results presented in this report focus on the single mode case.

Helicopters can encounter many different types of rotor dynamic instability during wind tunnel testing. Instability can arise from pure mechanical coupling as in ground resonance or from aerodynamic coupling in forward flight. Rotor blades are designed such that the rotor blade mode frequencies lie between multiples of the rotor normal operating RPM. This fact places the modes of interest between a known band of frequencies and allows isolation of these modes with the use of a bandpass filter. (This is in contrast to fixed wing flutter where the modal frequencies are not as well defined.) Prior knowledge of the approximate frequency band allows for pretest selection of the bandpass filter passband, which in turn permits automated use of the identification algorithm. The identification method identifies both damping and frequency of the modes within the preselected passband.

Recursive maximum likelihood methods for the identification of parameters from input/output data have been extensively researched (ref. 4 and ref. 5). However, the application to real-time identification of rotor blade damping has not been previously done. These real-time methods are based upon an input/output discrete transfer relationship or autoregressive moving average (ARMA) representation. This representation leads to a simple, accurate, and numerically efficient identification algorithm. Other methods for real-time identification of parameters such as least squares or instrumental variable produce either biased estimates in the presence of measurement noise or require extensive user pretuning for proper convergence. The recursive maximum likelihood procedure selected for the research reported herein has excellent convergence properties and requires no user pretuning. This technique is referred to as the RML2 method in reference 4 and reference 5.

Flutter boundary prediction has been performed in reference 6 for a fixed wing aircraft using nonrecursive maximum likelihood identification in conjuction with Jury's determinate method to predict the stability boundary. The present research differs from the techniques used in reference 6 in that recursive on-line maximum likelihood procedures are used. In addition, the objective in this research is to provide continuous on-line estimation of modal damping as wind tunnel testing is performed.

The real time identification procedure is described in this report. An

investigation is conducted using simulation data to determine the convergence characteristics of the algorithm and identification accuracy with random input excitation and measurement noise. The effect of bandpass filter bandwidth on identification accuracy is quantified. A lightly damped blade mode with 2% critical damping and moderately damped mode of 10% critical damping is used in the investigation. The algorithm is applied to hingeless rotor random response test data obtained from the NASA Langley Research Center Hover Test Facility. Test data is analyzed using the algorithm and damping and frequency estimates are compared with other available predictions.

SYMBOLS

a_j	coefficients of the characteristic equation for a dynamic system of order n, j = 1, n, also defined in equation 2.9
A	stability matrix appearing in linear state equation 2.5
A(z)	polynomial in the shift operator z^{-1}, $A(z) = 1 + a_1z^{-1} + a_2z^{-2} + \text{---} + a_nz^{-n}$
B'	control matrix appearing in linear state equation 2.5
b_i	coefficients associated with the control input in the ARMA representation
B(z)	polynomial in the shift operator z^{-1}, $B(z) = b_1z^{-1} + b_2z^{-2} + \text{---} + b_nz^{-n}$
B_1	cyclic control input to rotor, deg.
BW	filter bandwidth used in the digitial filter, Hz
c_i	coefficients associated with the innovations in the ARMA representation
C(z)	polynomial on the shift operator z^{-1}, $C(z) = 1 + c_1z^{-1} + c_2z^{-2} + \text{---} + c_nz^{-n}$
cov	covariance of the parameter estimate
$\overline{cov}$	covariance of the parameter estimate corrected for nonwhite innovations
e	natural logrithm basis, e = 2.71828
F_i	generalized force scaled by generalized inertia for the ith mode
G	control matrix appearing in the discrete state equation 2.7
H	measurement matrix appearing in the linear state equation 2.7
h_j	weights used in the digital filter
i	discrete data point index, also mode number index
j	complex variable $j = \sqrt{-1}$, also data sample shift index
K	Kalman filter gain
K_{t+1}	gain matrix used in the recursive maximum likelihood algorithm
L'	negative log likelihood function
L	likelihood function
M	number of data points on either side of current point fitered by the digital filter
M_i	vector of mode shapes at a radial station
N	number of data points
n	number of coefficients in ARMA model for a_i, b_i, c_i; i = 1,n
P_t	parameter covariance matrix used in the recursive maximum likelihood algorithm
P(0)	initial parameter covariance
1p	nondimensional rotor frequency
q_i	generalized rotor coordinate associated with ith mode
RMS	root mean square

system described by Eq. (2.3) and Eq. (2.4) (ref. 7) can be described in state form as

$$\dot{x} = A\,x + B'u \tag{2.5}$$

$$y = x_1 \tag{2.6}$$

where

$$A = \begin{bmatrix} -a_1 & 1 & 0 & -- \\ -a_2 & 0 & 1 & -- \\ \vdots & & \ddots & \\ -a_{n-1} & & & \ddots \\ -a_n & & & \end{bmatrix}$$

$$B' = \begin{bmatrix} b'_1 \\ b'_2 \\ \vdots \\ b'_{n-1} \\ b'_{n-2} \end{bmatrix}$$

and x is a n x 1 state vector of normalized coordinates and velocities, u is the single input and y is the single output.

In the presence of random process and measurement noise the continuous system Eqs. (2.5) and (2.6) can be represented by the discrete stochastic system of linear difference equations

$$\begin{aligned} x(i+1) &= \phi x(i) + Gu(i) + \Gamma w(i) \\ y(i) &= Hx(i) + v(i) \end{aligned} \tag{2.7}$$

where i is the index for the discrete sample time. The discrete time process noise w(i) and measurement noise v(i) are assumed to be zero mean white sequences with covariance matrices Q and R respectively.

By use of the Kalman Filtering theorem (ref. 8 and ref. 9) the stochastic model of Eq. (2.7) can be represented by an equivalent form as

$$\hat{x}(i+1) = \phi\,\hat{x}(i) + Gu(i) + K\nu(i)$$
$$y(i) = H\,\hat{x}(i) + \nu(i) \qquad (2.8)$$

where $\hat{x}(i)$ denotes the conditional mean of x(i) given measurements y(i-1), y(i-2), ..., and $\{\nu(i)\}$ is a sequence of independent equally distributed random variables with zero mean and covariance λ^2. The representation of Eq. (2.8) is an innovation representation (ref. 8 and ref. 9) of the process and the sequence $\{\nu(t)\}$ is called the innovations. In steady state the filter gain matrix K is constant and combined with the innovations covariance λ^2, replaces the noise statistics Q and R of Eq. (2.7). The innovations sequence $\nu(i)$ replaces both the process noise and measurement noise.

The innovation model of Eq. (2.8) takes on a particularly simple form for a single input-single output (SISO) model. The discrete SISO form or autoregressive moving average (ARMA) representation is obtained using the shift operator q^{-1}, where $q^{-1}x(i+1) = x(i)$. Application of the shift operator to Eq. (2.8) yields the SISO ARMA representation

$$\sum_{j=0}^{n-1} a_j y(i-j) = \sum_{j=1}^{n} \{b_j u(j-1) + c_j \nu(i-j)\} \qquad (2.9)$$

where a_o=1 and c_o = 1, n is the order of the autoregressive part, and also the order of the moving average part. In this description there is no concept of state and a n state vector produces n lags y(i-j), j=0, 1, 2,...n-1.

The ARMA representation of Eq. (2.9) provides a complete description of the SISO stochastic process of Eq. (2.7). The unknown parameters of the model in Eq. (2.9) are the parameter a_j, b_j, c_j and the scalar innovation covariance. The unknown parameter vector Θ is

$$\Theta = \{a_1, a_2, \ldots a_n, b_1, b_2, \ldots b_n, c_1, c_2, \ldots c_n\}^T \qquad (2.10)$$

along with the scalar innovation covariance denoted by λ^2. The left-hand side of Eq. (2.9) contains the coefficients of the characteristic equation.

The damping and frequency of the n-modes are obtained from the roots of the characteristic equation.

$$Z^n + a_1 Z^{n-1} + a_2 Z^{n-2} + \ldots a_n = 0 \qquad (2.11)$$

where Z is the discrete Z transform variable.

The general ARMA model given by Eq. (2.9) can thus be used to identify the coefficients a_j, j=1, n-1 of a general n^{th} order system from the single measurement y. The stability of the system is determined from the roots of the discrete characteristic equation. To obtain the continuous damping and frequency the mapping from the discrete z-transform domain to the continuous s-transform Laplace transform domain is then required.

The ARMA representation of Eq. (2.9) is more suitable for on-line identification than the complete state space model of Eq. (2.7) or the state innovations model of Eq. (2.8). The ARMA representation has fewer parameters and the noise statistics are completely characterized in the moving average part of Eq. (2.9) (i.e. the c coefficients) and innovation covariance λ^2. Thus in order to identify the coefficients of the characteristic equation (i.e. the a coefficients), it is also required to identify the c coefficients and innovation covariance λ^2. This then provides a complete description of the stochastic process, from which the modal damping and frequency can be determined. Also, if a known control input is applied the b coefficients of Eq. (2.9) must also be identified.

The overall identification procedure is shown in block diagram form in figure 1. The data y (and control input u(i) if available) is discretized and bandpass filtered to obtain the desired rotor blade modes. The filtered data is passed through the recursive maximum likelihood identification algorithm (discussed in the next section) and the identified parameters $\hat{a}_i$ represent the coefficients of the discrete characteristic equation. Discrete roots (eigenvalues) are computed from the characteristic equation. The modal damping and frequency are then obtained by transforming the discrete roots to the continuous Laplace transform domain. The RML algorithm computes both the parameters and standard deviations of the parameter estimates as noted in figure 1.

The discrete roots are obtained from the characteristic equation by use of any standard root finding algorithm of a polynomial equation. Transformation to the continuous domain is accomplished by defining the discrete complex root Z and continuous root s

$$Z = Z_R + j\, Z_I \tag{2.12}$$

$$s = \sigma + j\, \omega \tag{2.13}$$

and using the discrete to continuous transformation

$$e^{sT} = Z \tag{2.14}$$

where T represents the discrete sample time interval.

Substituting Eq. (2.12) and (2.13) into Eq. (2.14) yields

$$e^{\sigma T + j\omega T} = Z_R + j\, Z_I \tag{2.15}$$

Expressing Eq. (2.15) in terms of amplitude and phase and equating right and left hand sides yields

$$e^{2\sigma T} = Z_R^2 + Z_I^2 \tag{2.16}$$

$$\omega T = \tan^{-1} \frac{Z_I}{Z_R} \tag{2.17}$$

Taking the natural logrithm of Eq. (2.16) and solving for σ and ω in Eq. (2.16) and (2.17) yields the continuous damping and frequency

$$\sigma = \frac{1}{2T} \ln (Z_R^2 + Z_I^2) \tag{2.18}$$

$$\omega = \frac{1}{T} \tan^{-1} \frac{Z_I}{Z_R} \tag{2.19}$$

The undamped natural frequence ω_n and damping ratio ζ are related by

$$\zeta\omega_n = \sigma \tag{2.20}$$

$$\omega = \omega_n (1-\zeta^2)^{1/2} \tag{2.21}$$

The damping ratio and undamped natural frequency can be computed with the use of Eq. (2.18) through Eq. (2.21)

$$\omega_n = (\omega^2 - \sigma^2)^{1/2} \tag{2.22}$$

$$\zeta = \frac{\sigma}{\omega_n} \tag{2.23}$$

If there is only one mode, the root finding algorithm is not required and the damping and frequency can be obtained directly from the a coefficients a_1 and a_2 using

$$\sigma = \frac{1}{2T} \ln(1/a_2) \tag{2.24}$$

$$\omega = \frac{1}{T} \cos^{-1}(-a_1/2\sqrt{a_2}) \tag{2.25}$$

The next section describes the details of the recursive maximum likelihood identification algorithm for computing the coefficients of the ARMA represention of Eq. (2.9).

Recursive Maximum Likelihood Identification Algorithm

The origin of this method is based upon the off-line maximum likelihood method of Astrom-Bohlin (ref. 10). The recursive version is described in Söderstrom (ref. 11). This method is selected for the rotorcraft blade mode identification due to its excellent convergence properties. Reference 4 and Reference 5 describes the recursive version in comparison to other methods.

The off-line maximum likelihood version attempts to minimize the negative log likelihood function

$$L' = -\log L(\Theta,\lambda) = \frac{1}{2\lambda^2} \sum_{t=1}^{N} \varepsilon_t^2 + N/2 \log \lambda + N/2 \log 2\pi \tag{2.26}$$

where

$$\Theta = \{a_1, a_2, \ldots a_n, b_1, b_2 \ldots b_n, c_1, c_2, \ldots c_n\} \tag{2.27}$$

and λ^2 represents the innovation covariance. The ARMA model of Eq. (2.9) is rewritten using the operator C(z), A(z) and B(z)

$$C(z)\ \varepsilon_t = A(z)\ y_t - B(z)\ u_t\ ,\ t = 1,2,...N \tag{2.28}$$

where the innovations is denoted by ε_t and t denotes the discrete sample time.

Since the prediction error Eq. (2.28) is nonlinear in the parameters c, a iterative solution is required to minimize the likelihood function L'.

Optimization of L' with respect to λ^2 yields

$$\hat{\lambda}^2 = 1/N \sum_{t=1}^{N} \varepsilon_t^2 \tag{2.29}$$

Therefore maximum likelihood identification of θ is equivalent to minimization of

$$V(\theta) = \sum_{t=1}^{N} \varepsilon_t^2 \tag{2.30}$$

subject to the prediction error model

$$\varepsilon_t = [C(z)]^{-1}\ [A(z)\ y_t - B(z)\ u_t] \tag{2.31}$$

An approximate solution is obtained by linearization of ε_t

$$\varepsilon_t = \varepsilon(\hat{\theta}) + \frac{\partial \varepsilon}{\partial \theta}\ (\hat{\theta})\ (\theta - \hat{\theta}) \tag{2.32}$$

where the linearization is performed about the estimate $\hat{\theta}$.

Eq. (2.32) is a linear prediction error equation and therefore the minimization of Eq. (2.30) subject to Eq. (2.32) can be obtained using the recursive least square solution (ref. 12)

Therefore the recursive solution is

$$\hat{\theta}_{t+1} = \hat{\theta}_t + K_{t+1}\ \hat{\varepsilon}_{t+1} \tag{2.33}$$

$$K_{t+1} = P_t\ \bar{x}_{t+1}/(\lambda_c + \bar{x}_{t+1}^{-T}\ P_t\ \bar{x}_{t+1}) \tag{2.34}$$

$$P_{t+1} = [P_t - K_{t+1}\ \bar{x}_{t+1}^{-T}\ P_t\ ]/\lambda_c \tag{2.35}$$

where $\hat{\varepsilon}_{t+1}$ is computed from

$$x(t+1) = \begin{bmatrix} -\hat{c}_1 & 1 & \cdots & 0 \\ -\hat{c}_2 & 0 & \ddots & 0 \\ \vdots & \vdots & & \vdots \\ & & & 1 \\ -\hat{c}_n & & & 0 \end{bmatrix} x(t) + \begin{bmatrix} 1 \\ 0 \\ \vdots \\ 0 \end{bmatrix} y_{t+1} + \begin{bmatrix} \hat{a}_1 \\ \vdots \\ \hat{a}_n \end{bmatrix} y_t - \begin{bmatrix} \hat{b}_1 \\ \vdots \\ \hat{b}_n \end{bmatrix} u_t \qquad (2.36)$$

where $x_1(t) = \varepsilon(t)$.

The sensitivity $\bar{x}_{t+1} = \dfrac{\partial \varepsilon_{t+1}(\hat{\theta})}{\partial \theta}$ is computed according to

$$\bar{x}_{t+1} = \left[\begin{array}{cccc|cccc|cccc} -\hat{c}_1 & -\hat{c}_2 & \cdots & -\hat{c}_n & & & & & & & & \\ 1 & 0 & & & & & & & & & & \\ & \ddots & & & & & & & & & & \\ 0 & & & & & & & & & & & \\ & & 1 & 0 & & & & & & & & \\ \hline & & & & -\hat{c}_1 & -\hat{c}_2 & \cdots & -\hat{c}_n & & & & \\ & & & & 1 & 0 & & & & & & \\ & & & & & \ddots & & 0 & & & & \\ & & & & 0 & & \ddots & & & & & \\ & & & & & & 1 & 0 & & & & \\ \hline & & & & & & & & -\hat{c}_1 & -\hat{c}_2 & \cdots & -\hat{c}_n \\ & & & & & & & & 1 & 0 & & \\ & & & & & & & & & \ddots & & \\ & & & & & & & & 0 & & 1 & 0 \end{array}\right] \bar{x}_t - \begin{bmatrix} y_t \\ 0 \\ \vdots \\ 0 \\ -u_t \\ 0 \\ \vdots \\ 0 \\ -\hat{\varepsilon}_t \\ 0 \\ \vdots \\ 0 \end{bmatrix} \qquad (2.37)$$

The factor λ_c in Eq. (2.34) and (2.35) is used to improve convergence rate (ref. 4) and is obtained from

$$\lambda_c^{t+1} = C_o \lambda_c^t + 1 - C_o \qquad (2.38)$$

where $\lambda_c^o = .95$ and $C_o = .99$. The values of λ_c^o and C_o are the same as those used in reference 4 which were found to yield good convergence.

To track slowly time varying parameters the convergence factor λ_c is set to a constant value less than unity for all time. This is equivalent to exponential weighting of the least square criterion Eq. (2.30) and is fully discussed in reference 4.

Eqs. (2.33) through Eq. (2.38) constitutes the recursive maximum likelihood algorithm.

Bandpass Filter

The selection of the desired modes for identification is accomplished with a zero phase shift digital filter, due to Graham (ref. 13). This filter is not recursive but uses numerical convolution of the raw data to obtain the filtered data. This filter can be used in near-real time by shifting the filter weight function h_j one data point ahead as each new raw data point is received. The actual filtered output requires a finite segment of data ahead in time of the current data point being filtered. This results in a slight time delay before the estimated coefficients are available. Using a sample rate of .01 seconds this represents a delay of between 1 and 2 seconds before the filtered output is obtained. A recursive bandpass filter such as a n^{th} order Butterworth filter could be used to eliminate this delay, however the Graham filter was selected for the results presented here due to its excellent filter properties and availability. The 1 to 2 second delay was not considered significant for the real time monitoring of blade modes.

The filtered output y'_i at data point i obtained using the numerical convolution is

$$y'_i = \sum_{j=-M}^{M} h_j \, y_{j+i} \tag{2.39}$$

where y_{j+i} is the raw data which requires M data points ahead and M data points behind point i. The weight function h_j is computed from

$$h_j = \frac{\pi}{2jT} \; \frac{(\sin \omega_t jT + \sin \omega_c jT)}{\pi^2 - (\omega_t - \omega_c)^2 (jT)^2} \qquad j = -M, \ldots, +M \qquad j \neq 0 \tag{2.40}$$

and

$$h_j = \frac{\omega_t + \omega_c}{2\pi} \quad , \quad j = 0$$

The cutoff frequency ω_c and termination frequency ω_t are selected to achieve the desired passband about a center frequency of zero (low pass filter). The weights h_j are then normalized by the sum of all the weights. To achieve bandpass filtering about a center frequency ω_o, the weights are shifted by multiplication of h_j by $\cos \omega_o jT$. Eq. (2.39) and (2.40) describe the low pass filter (ref. 13) and the bandpass filter is obtained by multiplication of the weights h_j by $\cos \omega_o jT$ and is described in reference 14.

The use of the bandpass filter on both simulation data and test data is presented in the next section along with the recursive maximum likelihood identification results.

RESULTS FROM SIMULATION ANALYSIS

Before analysis of test data is performed it is important to assess the characteristics and limitations of the identification method by simulation. Of particular importance is the convergence characteristics. (i.e. the quantification of parameter accuracy as the data is processed) The amplitude of the random response, the initial parameter start-up, and the digital filter are investigated as to their effect on identified parameter accuracy. In addition, the standard deviation of the parameter estimate as computed in the algorithm must be evaluated as to its validity as a measure of identified parameter accuracy.

Simulation Model

The model used in the simulation analysis is intended to represent two situations. First, a moderately damped mode (ζ = 10% critical damping) representative of an articulated rotor or highly damped hingless rotor is investigated. Second, a lightly damped mode (ζ = 2% critical damping) representation of a hingless rotor is investigated. In both cases, the simulation model represents a single uncoupled mode. Such a mode can occur as an isolated blade mode or a lightly damped "system" mode such as the in-plane regressing mode typical of ground resonance. Although the identification procedure is applicable to any number of coupled modes, the results presented are for the single mode case which is perhaps the most important for rotor stability assessment. In addition, the modal identification procedure can be repeated any number of times on the same data, in each case a different mode isolated with the bandpass filter.

The model used in the simulation is a state space second order system and is represented by

$$\dot{x}_1 = x_2 \tag{3.1}$$

$$\dot{x}_2 = -\omega_n^2 x_1 - 2\zeta\omega_n x_2 + w(t) \tag{3.2}$$

where x_1 is the blade modal response and w(t) is zero-mean white gaussian process noise.

The modal measurement is obtained from

$$y = x_1 + r \tag{3.3}$$

where, r is zero-mean white gaussian measurement noise.

The stochastic model given by Eq. (3.1) through Eq. (3.3) is simulated in discrete form by

$$x_1(i+1) = x_1(i) + x_2(i)\ \overline{\Delta t} \tag{3.4}$$

$$x_2(i+1) = -\omega_n^2\ \overline{\Delta t}\ x_1(i) + (1-2\zeta\omega_n\ \overline{\Delta t})\ x_2(i) + w_d(i)$$

and $$y(i) = x_1(i) + r(i) \tag{3.5}$$

where w_d is zero-mean white discrete process noise and r is zero-mean white discrete measurement noise.

In order to obtain acceptable integration accuracy using the discrete model of Eq. (3.4) and Eq. (3.5), the integration step size $\overline{\Delta t}$ should be at least 10 times smaller than the data sample time between the i and i+1 sample. For all simulation runs $\overline{\Delta t}$ was selected as $\overline{\Delta t}$ = .002 seconds and the measurement y(i) was made every Δt = .02 seconds.

The maximum likelihood algorithm identifies the coefficients of the equivalent ARMA representation as discussed in the previous section. The ARMA representation used is

$$y_i + a_1 y_{i-1} + a_2 y_{i-2} = c_1 \nu_{i-1} + c_2 \nu_{i-2} + \nu_i \tag{3.6}$$

As discussed previously, Eq. (3.6) is a single input-single output discrete model and is equivalent to an innovations or Kalman filter representation of the system described by Eq. (3.4) through Eq. (3.5). The filter gains are embedded in the c coefficients of Eq. (3.6). The a coefficients are the coefficients of the characteristic equation from which the damping, ζ, and frequency, ω_n, can be computed as shown in Eq. (2.20) through Eq. (2.25) of the previous section.

Moderate Damping Case, ζ = 10%, ω_n = 23.15 rad/sec

The simulation model shown by Eq. (3.4) and Eq. (3.5) was used to generate 5000 data samples. The measurement noise standard deviation used is σ_r = .1 and various levels of process noise were investigated. The data used in the identification algorithm is unfiltered. The initial parameter start-up is

$$\theta(0) = \{-1.5 \quad .80 \quad 0. \quad 0.\} \tag{3.7}$$

The parameter a_2 = .80 represents a critical damping of greater than 20%. The initial parameter covariance used is

$$P(0) = \{.1 \quad .1 \quad 1.0 \quad 1.0\} \tag{3.8}$$

Three different levels of process noise were simulated (σ_w = 1.0, .2, and .04). This corresponds to a state response with RMS levels of 1.25 deg, .25 deg, and .05 deg, respectively. Identified parameter convergence is shown in figure 2 through figure 4 for the three levels of random excitation. As shown in the figures, convergence to the true parameter values occurrs in each case, with slower convergence achieved for the smaller levels of process noise excitation. The ARMA coefficients are shown on the left hand scale and the damping ratio is shown on the right hand scale of the plot for coefficient a_2. The damping ratio is computed according to

$$\hat{\zeta} = \frac{1}{2\omega_n \Delta t} \ell n(1/\hat{a}_2) \tag{3.9}$$

The identified c coefficients account for the presence of measurement noise. If the ratio of process to measurement noise is large as in figure 2 (σ_w^2/σ_r^2 = 100),

then the c coefficients are small. As the ratio σ_w^2/σ_r^2 decreases, the c coefficients increase in magnitude as shown in figure 4. In the limit as σ_w^2/σ_r^2 approaches ∞, then $\hat{c}$ approaches zero, which reduces to a least square estimator for the a coefficients. Thus, the c coefficients in the maximum likelihood method accounts for the presence of both measurement and process noise by automatically "tuning" the Kalman filter in proportion to the ratio of process to measurement noise.

Effect of Initial Parameter Estimate. The parameter identification results just presented for the 10% critical damping case is repeated for different initial parameter estimates. The second set for the initial parameter estimate and covariance is

$$\theta(0) = \{0 \quad 0 \quad 0 \quad 0\} \tag{3.10}$$

$$P(0) = \{1.0 \quad 1.0 \quad 1.0 \quad 1.0\} \tag{3.11}$$

The identified parameter convergence is shown in figure 5 and figure 6 for process noise levels of $\sigma_w = .2$ and $\sigma_w = .04$, respectively. Again, identified parameter convergence is excellent. In all cases studied the final convergence was found to be independent of the initial parameter start-up.

Lightly Damped Case, $\zeta = 2\%$, $\omega_n = 23.15$ rad/sec

The simulation was repeated using a critical damping of $\zeta = 2\%$. This case is representative of a lightly damped hingeless rotor. Two levels of process noise were used ($\sigma_w = .2$ and $\sigma_w = .04$). This random excitation produces a RMS random response of .75 deg and .15 deg, respectively. The identified parameter convergence for these two cases is shown in figure 7 and figure 8. Parameter convergence is excellent and occurs more rapidly than for the 10% damping case (compare fig. 7 with fig. 3 and fig. 8 with fig. 4). The RMS of the random response is larger for the low damping case, as is expected, and the damping is more rapidly identified.

Data Length Required For Accurate Identification

Based upon the limited number of simulation runs performed an estimate of the number of data samples required for accurate identification can be approximated. As was shown in the simulation study, the required data length for convergence depends on the process noise level and damping value. Since the actual process noise level is not known in a wind tunnel test program, the RMS amplitude of the random response is presented rather than process noise level (σ_w). Figure 9 presents a graphical summary of the simulations performed and shows the number of data samples required to identify damping ratio (% critical) to within 10% error. This is plotted vs the RMS amplitude of random response in degrees. Two different damping ratios ($\zeta = 10\%$ and $\zeta = 2\%$) are presented. The results shown in figure 9 are obtained for a measurement noise level of $\sigma_r = .1$ degrees, $\omega_n = 23.15$ rad/sec, and $\Delta t = .02$ seconds sample time interval.

The number of samples required is very dependent upon the RMS amplitude and the damping ratio. Typically, the number of samples required ranges from 1000 samples for low damping (2%) and large RMS amplitude response (1.25 deg) to greater than 5000 samples for high damping (10%) and low RMS response (.05 degrees). The

results in figure 9 should be used only as a guide since the results are presented for one value of measurement noise (σ_r = .1), using unfiltered data, and a sampling rate of Δt = .02 seconds.

The results of figure 9 show that identified parameter convergence requires between 20 seconds to 100 seconds of data (Δt = .02) depending upon the amplitude of random response and system damping level. A significant finding is that damping can be accurately identified from random response levels as low as .05 degrees in the presence of .1 degrees measurement noise. The smaller the RMS response, the more data samples required for parameter convergence.

Digital Filter Selection

A bandpass filter is required to remove unwanted modes and 1 per rev contaminations from the data before identification is performed. This section demonstrates the effect of the bandpass filter on identification accuracy for various filter designs. Figure 10 shows the amplitude vs. frequency characteristics of four digital filters used to separate the desired mode. The mode of interest, ω_ζ, occurs at 3.68 Hz (23.15 rad/sec) and the 1 per rev (1p) signal is shown at 11.17 Hz. Filter number 1, 2 and 4 of figure 10 are bandpass filters, whereas filter number 3 is a low pass filter.

The simulation data was generated with a process noise level of σ_w = .2 for the 2% critical damping case. Four separate runs were made and identified parameter convergence was assessed. Figure 11 shows identified parameter convergence for filter number 4. The identified damping value is somewhat biased from the true value of ζ = 2%. Filter number 1, 2 and 3 showed a larger bias, indicating that some of the signal (i.e. the random response) was removed by the filter. The smaller the filter bandwidth, the more signal removed and thus, the larger the error. Figure 12 shows the effect of filter bandwidth on identified damping ratio for the four filters used.

It is shown that a filter bandwidth between 8 and 10 Hz is required to achieve acceptable accuracy. Normalizing the frequency by the natural frequency, the following approximate frequency range should be selected for the filter assuming a white noise random excitation

$$.27\omega_\zeta \leq \omega \leq 2.4\omega_\zeta \tag{3.12}$$

The relationship in Eq. (3.12) is approximate and in practice the filter bandwidth should be chosen as large as possible within the 0 to 1p frequency band for modes below 1 p. For modes above 1p but below 2p the filter should be selected between 1p and 2p frequencies.

For a mode which lies very close to the 1p frequency, it may be required to remove the 1p frequency with a separate estimator before using the bandpass filter.

Figure 11 shows that the identified a coefficients are somewhat biased by the filter. The c coefficients are significantly biased. This is because the c coefficients are influenced by the ratio of process noise to measurement noise which assumes the random noise is white noise. Since filtering produces colored innovations, this is reflected in the identified c coefficients.

Covariance of the Parameter Estimates

Real time identification of modal damping and frequency is not complete without knowledge of the uncertainty in the parameter estimate. The recursive maximum likelihood algorithm provdies a measure of the parameter covariance by use of the Cramer-Rao lower bound. A discussion of theorems relating the accuracy of maximum likelihood estimate to the Cramer-Rao lower bound is given in reference 12. The Cramer-Rao bound is a lower bound on estimation accuracy which is achieved by the maximum likelihood estimator asymptotically. An estimate of the parameter covariance is obtained by

$$\underset{N\to\infty}{\text{cov}}(\hat{\Theta}_N) = P_N \hat{\lambda}_N^2 \tag{3.13}$$

where P_N is obtained from Eq. (2.35) and the innovations covariance is computed from

$$\hat{\lambda}_N^2 = \frac{1}{N} \sum_{i=1}^{N} \nu_i^2 \tag{3.14}$$

Since, in practice, the noise characteristics of the innovations is often found to be "colored" rather than white, the parameter covariance as given by Eq. (3.13) must be corrected for non-white innovations (ref. 15). This can be accomplished using

$$\overline{\text{cov}}(\hat{\Theta}) = \text{cov}(\hat{\Theta}) \cdot \left(\frac{1}{2\ BW\ \Delta t}\right) \tag{3.15}$$

where, $\overline{\text{cov}}(\hat{\Theta})$ is the covariance corrected for non-white innovations and BW is the bandwidth of the colored noise which is set equal to the digital filter bandwidth of the bandpass filter used on the data. The correction term is approximate and is found to work well in practice as discussed in reference 15.

Since cov $(\hat{\Theta})$ represents the covariance of the coefficients of the characteristic equation, a transformation is required to obtain the covariance of the damping. Since the damping ratio is related to the coefficient a_2 by

$$\hat{a}_2 = e^{-2\hat{\zeta}\hat{\omega}_n \Delta t} \tag{3.16}$$

the covariance of $\hat{\zeta}$ can be obtained by linearization of Eq. (3.16) to first order as

$$\hat{a}_2 = 1 - 2\hat{\zeta}\hat{\omega}_n\ \Delta t \tag{3.17}$$

The covariance of $\hat{\zeta}$ can then be computed from Eq. (3.17) or

$$\text{cov}(\hat{\zeta}) = \overline{\text{cov}}(\hat{a}_2)/(2\ \ \Delta t\ \hat{\omega}_n)^2 \tag{3.18}$$

The standard deviation of $\hat{\zeta}$ is thus

$$\sigma_{\hat{\zeta}} = \frac{\sqrt{\overline{\text{cov}}(\hat{a}_2)}}{2\ \Delta t\ \ \hat{\omega}_n} \tag{3.19}$$

Eq. (3.15) is used to compute the standard deviation of the parameters in the ARMA model (e.g. the a- coefficients) and Eq. (3.19) is used to estimate the standard deviation of the estimated damping. Figure 13 shows the identified parameter convergence and standard deviation of the estimate for $\hat{a}_1$ and $\hat{a}_2$ for a simulation damping ratio of 2% and $\sigma_w = .2$. The estimated standard deviation provides an excellent measure of uncertainties for the identified parameters. Figure 14 shows identified parameter convergence and $\pm 2\sigma$ bands for a simulation damping of 2% with process noise $\sigma_\omega = .04$. The 1σ bands were slightly optimistic while the 2σ bands always contains the true damping value. Convergence is slower for figure 14 than figure 13 due to the smaller RMS of the random response ($\sigma_w = .04$ vs $\sigma_w = .2$). In all simulation studies performed the $\pm 1\sigma$ band or $\pm 2\sigma$ band provided an accurate measure of the parameter uncertainty.

RESULTS FROM TEST DATA

Test Data Description

A limited amount of test data obtained from a 4-bladed hingeless rotor test in the NASA Langley Research Center (LRC) Helicopter Hover Facility in 1981 was furnished by Mr. William T. Yeager, Jr. and Mr. Wayne R. Mantay. This data is used to identify in-plane mode damping and frequency. The rotor was operated in hover on the Aeroelastic Rotor Experimental System (ARES) over a rotor speed range of 0 to 618 RPM. The Helicopter Hover Facility is used for hover testing on the ARES before testing in the LRC Transonic Dynamics Wind Tunnel. Two RPM conditions, 250 RPM and 618 RPM, were investigated.

Of particular concern during rotor speed increase is the potential for ground resonance which occurs near the rotor in-plane regressing mode frequency ($\Omega-\omega_\zeta$). Since the in-plane lead-lag angle measurement occurs in the rotating system the bandpass filter was chosen to be centered around the rotating in-plane frequency ω_ζ. The 250RPM condition was observed to have a large resonance close to the rotor RPM, excited purely by random turbulence. The in-plane magnitude response was approximately $\pm$ 1 degree. Because of this large resonance the damping was expected to be quite small and a forced control input excitation would be dangerous to apply. The recursive maximum likelihood approach to identify modal damping from random response is thus ideally suited for this RPM condition.

The 618 RPM condition was considerably more damped and the modal response due to inherent random excitation was less than .05 degrees. It is expected that a longer data record length would be required for the 618 RPM condition for accurate identification because of the small amplitude response.

The test data used for the 250 RPM and 618 RPM conditions are shown in figure 15. Figure 15 shows only a portion of the 50 seconds of test data record length used in the identification. The lead-lag measurement for the 250 RPM case of figure 15 shows the $\pm$ 1 degree resonance response occurring at in-plane frequency ω_ζ. The sinusoidal response shown in figure 15 (bottom figure) for the measurement of lead-lag at the 618 RPM condition is due to the 1p frequency of the rotor and is <u>not</u> the in-plane mode. The large 1p response occurs at this condition due to a non-zero trim collective and cyclic control ($\Theta_o = 8^o$, $B_1 = 4^o$). The in-plane mode amplitude is less than .05 degrees which will be discussed in more detail later.

Identification Results at 250 RPM

The data at the 250 RPM condition shown in figure 15 (top figure) was processed with bandpass filter number 4, the characteristics of which are shown in figure 10. During the process of transforming the analog data tape to digital format a portion of the data was distroyed. The region of bad data occurred between the 1200th and 1600th samples. The complete data length processed consisted of 2500 samples at .02 seconds per sample rate.

The filtered data was used in the recursive maximum likelihood algorithm and the ARMA model coefficients identified. The results are shown in figure 16 for

the coefficients of the characteristic equation, $\hat{a}_1$ and $\hat{a}_2$ and the damping and frequency estimates are shown in figure 17. The region of bad data shown in these figures was also recursively processed by the algorithm. Identified parameter convergence is more accurate before the bad data region is encountered (i.e. up to 1200 samples).

Convergence is shown to be excellent in figure 16 and 17 as indicated by the $\pm$ 2σ accuracy bands shown in the figure before the region of bad data is encountered. The identified damping ratio at 1200 samples is 1.4% with 1 standard deviation equal $\pm$ .7%. The rapid convergence rate is a result of the large amplitude random response ($\pm$ 1 degree) as observed in the test data. The convergence rate shown in figure 16 and 17 is consistent with that expected from the simulation studies. For example, referring to figure 9, it is shown that perhaps 1500 data points are required to achieve the desired accuracy. Ideally, it would be desirable to process the full 2500 samples of data, however, because of the bad data region, the parameter estimate was shifted as shown in figure 16 and 17. Notice however, even with bad data, the algorithm is performing properly, in that the parameter estimates are attempting to recover as good data becomes available.

The identified frequency is shown in figure 17 and the estimated value at 1200 samples is 26.3 rad/sec. This value is nearly the same as determined by that obtained from shake test data and analytic predictions.

The identified damping and frequency parameters shown in figure 17 demonstrates that the identification procedure is performing successfully, and is in excellent agreement to that obtained in the simulation studies.

Identification Results at 618 RPM

The hover test data obtained at the 618 RPM condition is shown again in figure 18 with an expanded scale. Figure 18 shows the unfiltered data (top figure) and the bandpass filtered data (lower figure). The unfiltered data shows the dominant response is the 1p rotor frequency ($\pm$ .3 degrees). The filtered data removes the 1p frequency and retains the desired inplane mode which occurs at ω_ζ = 38.83 rad/sec. This mode is clearly shown in the lower figure of figure 18. The frequency of this mode appears to change frequency throughout the data length and is due to the random excitation driving the rotor system. The RMS amplitude of response is approximately .03 degrees as shown in the lower figure. Referring back to figure 10, the simulation study has shown that 5000 data points at a sample rate of .02 seconds (100 seconds of data) are required for acceptable accuracy for a RMS random response of .05 degrees. Since only 45 seconds of data are available at the 618 RPM condition and the RMS amplitude is .03 it is expected that convergence would require approximately twice as much data. This was in fact the case and the convergence plots are shown in figure 19. The identified damping ratio $\hat{\zeta}$, is shown in the lower figure and the $\pm$ 2σ accuracy band shows a longer data record is required for convergence. The identified damping is estimated after 45 seconds of data (4500 samples at .01 seconds sample rate) to be $\hat{\zeta}$ = 9% with 1 standard deviation of $\pm$ 3.5%. Independent estimates of the damping at this condition using the log decrement approach (visual inspection of an initial condition decay response was used) during the hover tests reveal a damping estimate of approximately 4%. The results of figure 19 thus contain this value within the accuracy band ($\pm$ 2σ) as shown in this figure.

The identified frequency convergence is also shown in figure 19 (top figure) and the estimated frequency is $\hat{\omega}$ = 38.83 radians/sec. This value is close to that obtained from independent shake test data and analytic predictions. The frequency parameter is identified more rapidly than the damping and requires less data length. This was found to be the case in the simulation study performed prior to analyzing the test data.

The identification results at the 618 RPM condition have correctly identified the frequency and approximately twice the data length available is required to identify the damping with acceptable accuracy. This conclusion was predicted by the simulation studies which show that 100 seconds of data is needed (twice the data length available) to obtain the required accuracy of the damping estimate.

Table 1 provides a summary of the identified damping and frequency at both the 250 and 618 RPM conditions. Comparisons are made with other available prediction methods. Shake test data and analytic simulation is referred to in the table as Analytic Method. The Log Decrement method is based upon visual inspection of the amplitude decay resulting from removal of a forced excitation. The damping values obtained from the Analytic method are estimates based upon the estimated rotor blade damping. The actual rotor blade damping value was not precisely known (1% critical damping was used in the simulation). The fixed system damping and frequency are for the in-plane regressing mode and the rotating system values are shown for the maximum likelihood method and log decrement method. The fixed system values are shown for the analytic method and rotating system values are obtained via transformation as noted in the table. From the data available at the 250 RPM and 618 RPM condition the recursive maximum likelihood approach performed as expected from the simulation studies.

Identified damping convergence to acceptable accuracy depends upon the magnitude of the RMS random response and the level of modal damping. The larger the random response the faster convergence. Typically from 30 to 100 seconds of data are required for acceptable accuracy. For $\pm$ 1 degree random response and low damping (1.4%) 30 to 50 seconds of data are required (250 RPM condition). For $\pm$ .03 degree random response and damping approximately 4%, approximately 100 seconds of data are required (618 RPM condition).

CONCLUSIONS

A recursive maximum likelihood identification procedure has been presented for the estimation of helicopter rotor blade modal damping and frequency from random response data. The algorithm was shown to have excellent convergence properties, provide accurate estimates of parameter covariance, and require virtually no user interaction. As a result, the RML method can be used for continuous estimation of damping and frequency during wind tunnel (or flight) testing.

Simulation studies have demonstrated that convergence to true parameter estimates occur even for very small amplitude RMS random response. RMS random response amplitude of .05 degrees to 1.25 degrees, which are typical of that expected in wind tunnel data, resulted in successful identification. Data record lengths required for accurate identification range from 20 seconds to 100 seconds of data depending upon RMS amplitude of random response and damping level. These data lengths are compatible with typical wind tunnel test data taken at steady rotor trim conditions. Since a forced input is not required, damping and frequency can be identified without interfering with other wind tunnel test objectives. The estimated parameter covariance was shown to provide accurate confidence bands on the damping, thus providing a indicator as to length of data required at a given test condition. Since identification parameter convergence was shown to be independent of initial parameter start-up values, the RML procedure can be used with virtually no user interaction. This proved to be the case on all data processed in this investigation.

The hover facility test data identified parameter convergence results obtained were consistent with the simulation studies. At 250 RPM, identified in-plane mode parameters are $\hat{\zeta}$ = 1.4% critical damping and $\hat{\omega}_\zeta$ = 26.3 rad/sec. The $\pm$ 1σ estimate on $\hat{\zeta}$ is .7% using 24 seconds of data. The identified frequency is in agreement with independent shake test data results. Accurate estimates of damping from other independent tests were not available. At 618 RPM, the identified frequency was $\hat{\omega}_\zeta$ = 38.83 rad/sec which is in agreement with independent shake test data. The identified damping is estimated using 45 seconds of data to be $\hat{\zeta}$ = 9% with $\pm$ 1σ = 3.5%. The large standard deviation shows that a longer data record is required which is consistent with the simulation results which showed that twice the data length is needed to obtain an accurate estimate. For both the 250 RPM and 618 RPM the RML identified parameter convergence performed as predicted by the simulation studies.

RECOMMENDATIONS

The emphasis of this investigation was on a single mode response separated from other modes with a bandpass filter. Although the techniques developed are applicable to any number of over-lapping modes, simulation studies on test data analysis have only been performed on a single mode case. Since rotorcraft rotor instability can result from coupled modes it is recommended that simulation studies analogous to that performed in this report be repeated for coupled mode response of two and possibly three modes. In addition, criteria should be investigated to automatically determine the required number of modes in the data.

The RML technique contains provision to track time varying parameters. Simulations should be performed to quantify this capability. This would be useful for monitoring damping changes while going from one steady rotor trim condition to another trim condition. The RML technique contains provision for identification of data generated by known forced control inputs and free response data. Both these situations have not been investigated via simulation. Simulation studies should be performed to quantify this capability.

Finally, further test data applications should be performed. Both on-line and off-line applications would provide a data base for further assessment of the RML technique.

REFERENCES

1. Hammond, C. E. and Doggett, R., Determination of Subcritical Damping by Moving - Block/Randomdec Applications. Flutter Testing Techniques. NASA SP-415, 1976, pp. 59-76.

2. Warmbrodt, W. and McCloud, J., Full-Scale Wind Tunnel Test of the Aeroelastic Stability of a Bearingless Main Rotor, Proceedings of the 37th Annual Forum of the American Helicopter Society, May 1981, pp. 204-216.

3. Bilger, J. M., Marr, R. L. and Zahedi, A., Results of Structural Dynamic Testing of the XV-15 Tilt Rotor Research Aircraft, Proceedings of the 37th Annual Forum of the American Helicopter Society, May 1981, pp. 493-502.

4. Soderstrom, T., Ljung, L. and Gustavsson, I., A Comparative Study of Recursive Identification Methods, Lund Institute of Technology Department of Automatic Control, Report 7427, Dec. 1974.

5. Soderstrom, T., Ljung, L. and Gustavsson, I., A Theoretical Analysis of Recursive Identification Methods, Automatica, Vol. 14, No. 3, May 1978.

6. Matsuzaki, Y. and Yasukatsu, A., Estimation of Flutter Boundary from Random Responses Due to Turbulence at Subcritical Speeds, Journal of Aircraft, Vol. 18, No. 10, 1981.

7. Astrom, K. J. and Eykhoff, P., System Identification - A Survey, Automatica, Vol. 7, pp. 123-162, 1971.

8. Kailath, T., An Innovations Approach to Least Squares Estimation - Parts I and II, IEEE Transaction on Automatic Control, Dec. 1968, pp. 646-661.

9. Mehra, R. K., Identification of Stochastic Linear Dynamic Systems Using Kalman Filter Representation, AIAA Journal, Vol. 9, No. 1, Jan. 1971.

10. Astrom, K. J. and Bohlin, T., Numerical Identification of Linear Dynamic Systems From Normal Operating Records, IFAC Symposium on Self-Adaptive Systems, Teddington, England, 1965.

11. Soderstrom, T., An On-Line Algorithm for Approximate Maximum Likelihood Identification of Linear Dynamic Systems, Report 7308, Div. of Automatic Control, Lund Institute of Technology, 1973.

12. Goodwin, G. C. and Payne, R. L., Dynamic System Identification: Experiment Design and Data Analysis, Academic Press, Inc. 1977.

13. Graham, R. J., Determination and Analysis of Numerical Smoothing Weights, NASA TR-179, Dec. 1963.

14. Ormsby, J. F. A., Design of Numerical Filters with Application to Missile Data Processing, Journal of the Association for Computing Machinery, Vol. 8, No. 3, July 1961.

15. Maine, R. E. and Iliff, K. W., Use of Cramer-Rao Bounds on Flight Data with Colored Residuals, Journal of Guidance and Control, Vol. 4, No. 2, March - April 1981.

Table 1. - Test Data Identified Damping and Frequency and Comparisons with Analytic and Log-Decrement Predictions

Estimation Method	Rotating System		Fixed System	
	ω_{ζ_R} Rad/Sec	ζ_R % Critical	ω_{ζ_F} Rad/Sec	ζ_F % Critical
Ω = 250 RPM				
Analytic Method(1)	26.2(3)	0.55%(4)	.8	18%
Log Decrement	- Not Used(5) -		---	---
Max. Likelihood	26.3	1.4%(1σ=.7%)	---	---
Ω = 618 RPM				
Analytic Method(6)	37.63(3)	0.33%(4)	25.9	.5%
Log Decrement(2)	--	4%	---	---
Max. Likelihood	38.83	9%(1σ=3.5%)	---	---

(1) Based upon analytic simulation and shake test data.

(2) Computed based upon visual inspection of amplitude decay response resulting from removal of forced excitation.

(3) Computed from shake test data.

(4) Computed from $\zeta_R = \zeta_F \frac{\omega_{\zeta_F}}{\omega_{\zeta_R}}$

(5) Forced excitation not used at 250 RPM because of large observed resonance at this condition.

(6) Values shown are obtained at slightly different RPM.

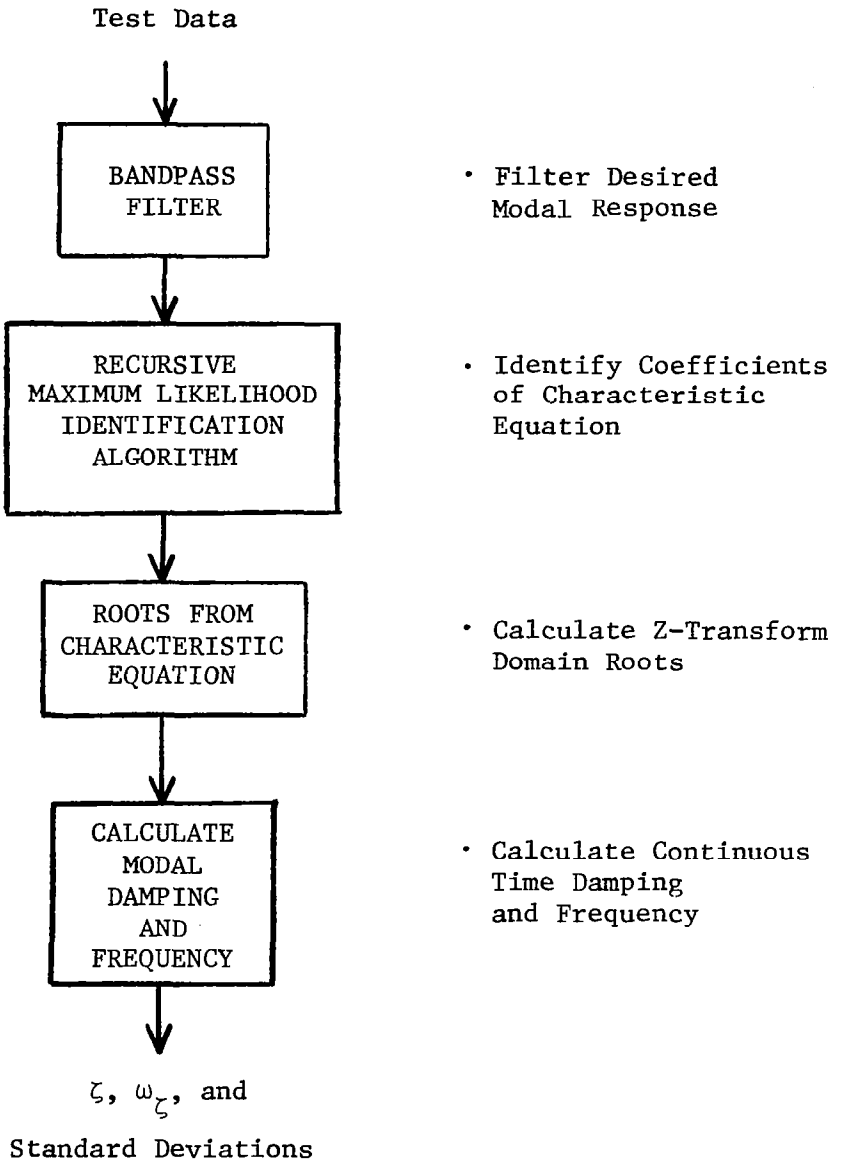

Figure 1. - Overall Procedure for Real Time Identification of Modal Damping and Frequency.

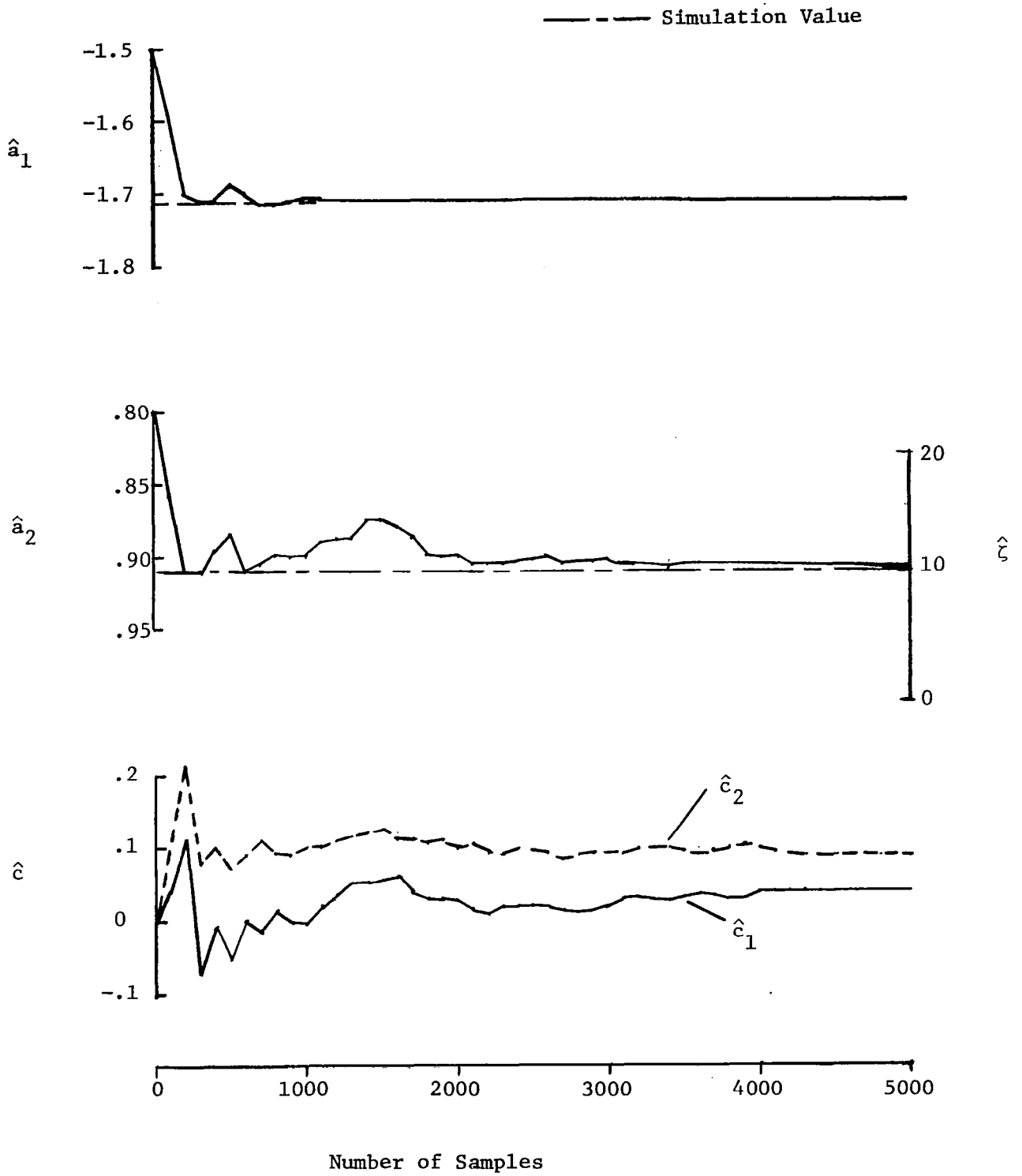

Figure 2. - Identified Parameter Convergence (RMS of Random Response = 1.25 deg, σ_r=.1 deg, σ_w=1.0 deg/sec^2, Δt=.02 sec, ω_n=23.15 rad/sec, ζ=10%).

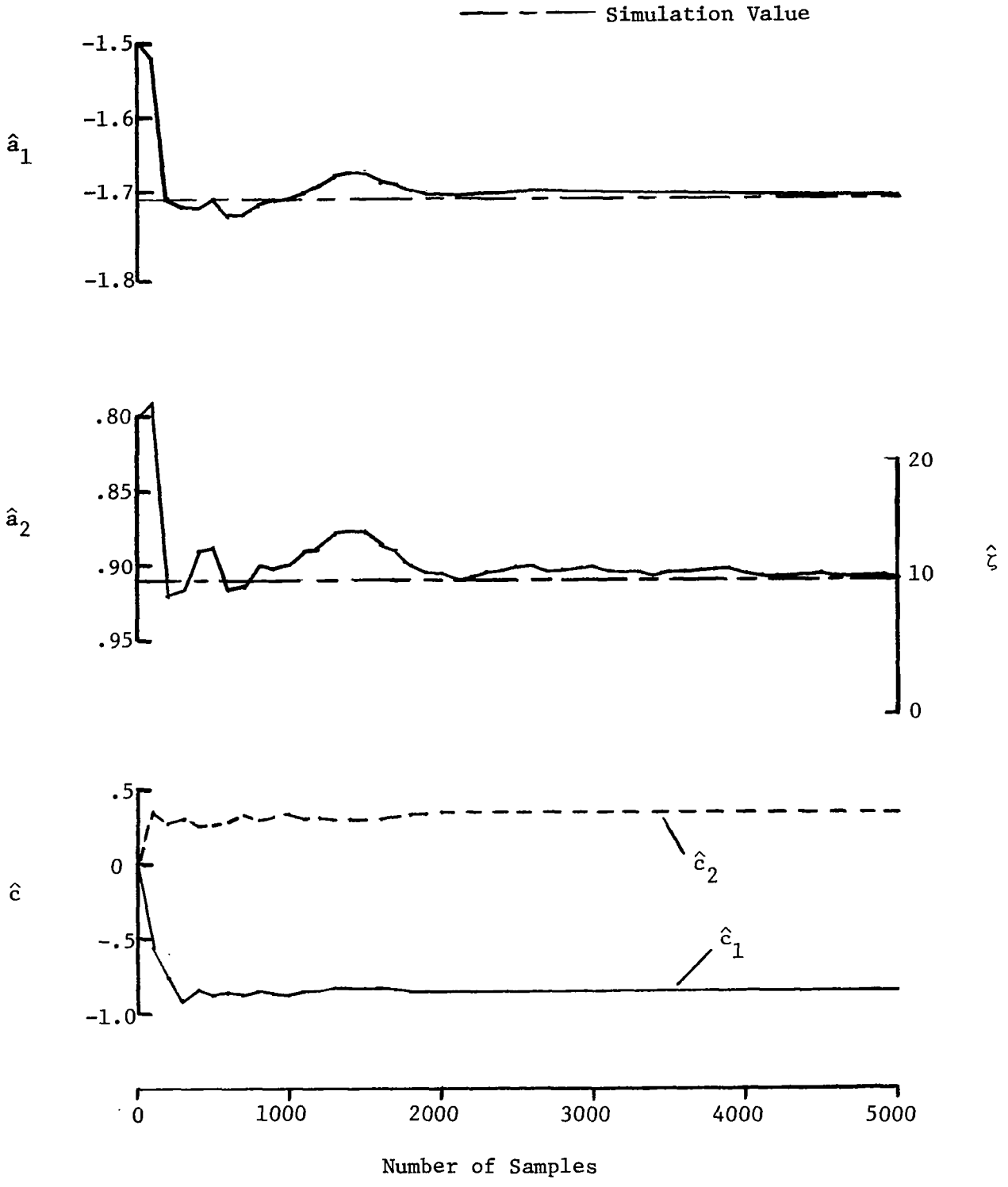

Figure 3. - Identified Parameter Convergence (RMS of Random Response = .25 deg, σ_r=.1 deg, σ_w=.2 deg/sec^2, Δt=.02 sec, ω_n=23.15 rad/sec, ζ=10%).

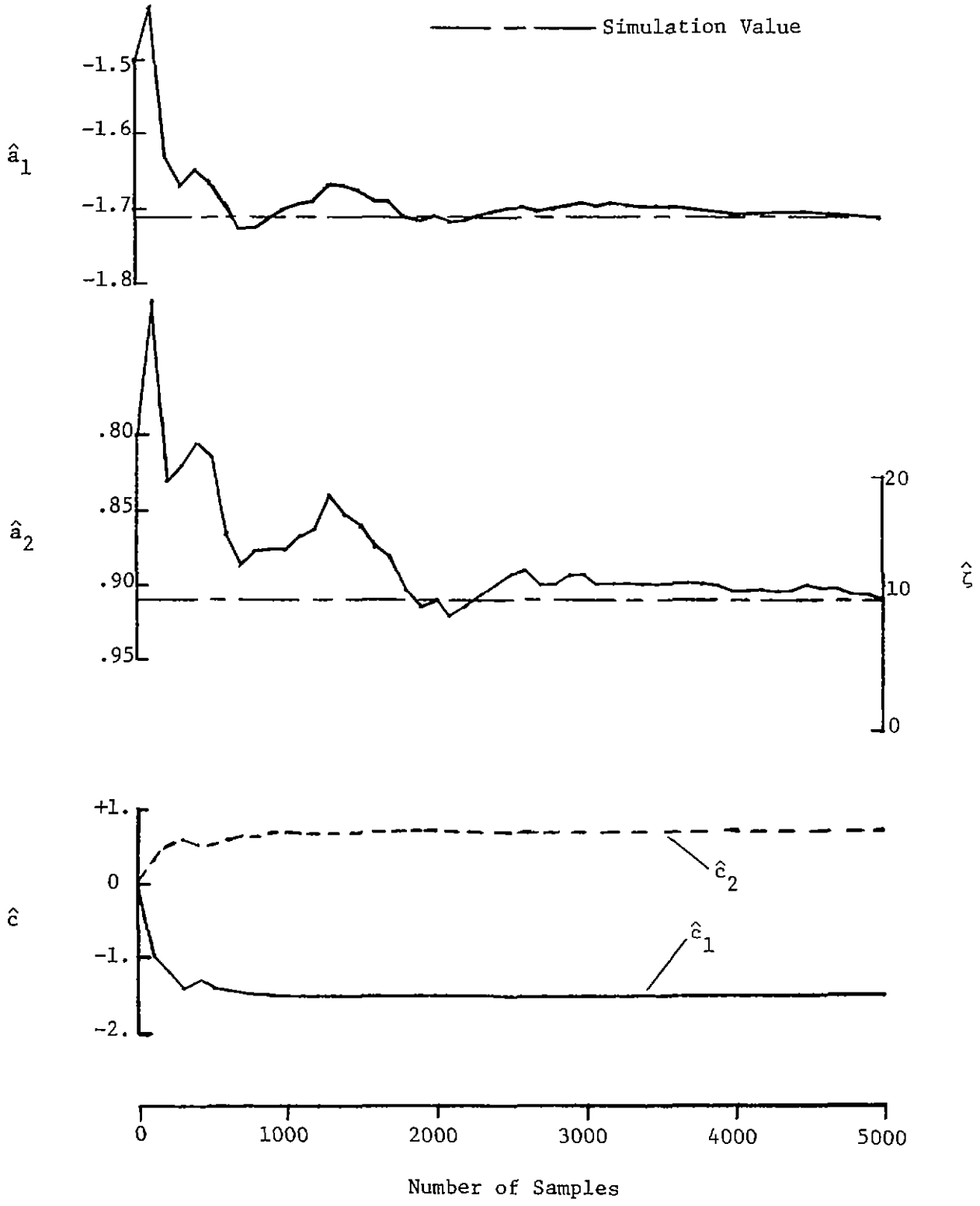

Figure 4. - Identified Parameter Convergence (RMS of Random Response = .05 deg, σ_r=.1 deg, σ_w=.04 deg/sec^2, Δt=.02 sec, ω_n=23.15 rad/sec, ζ=10%).

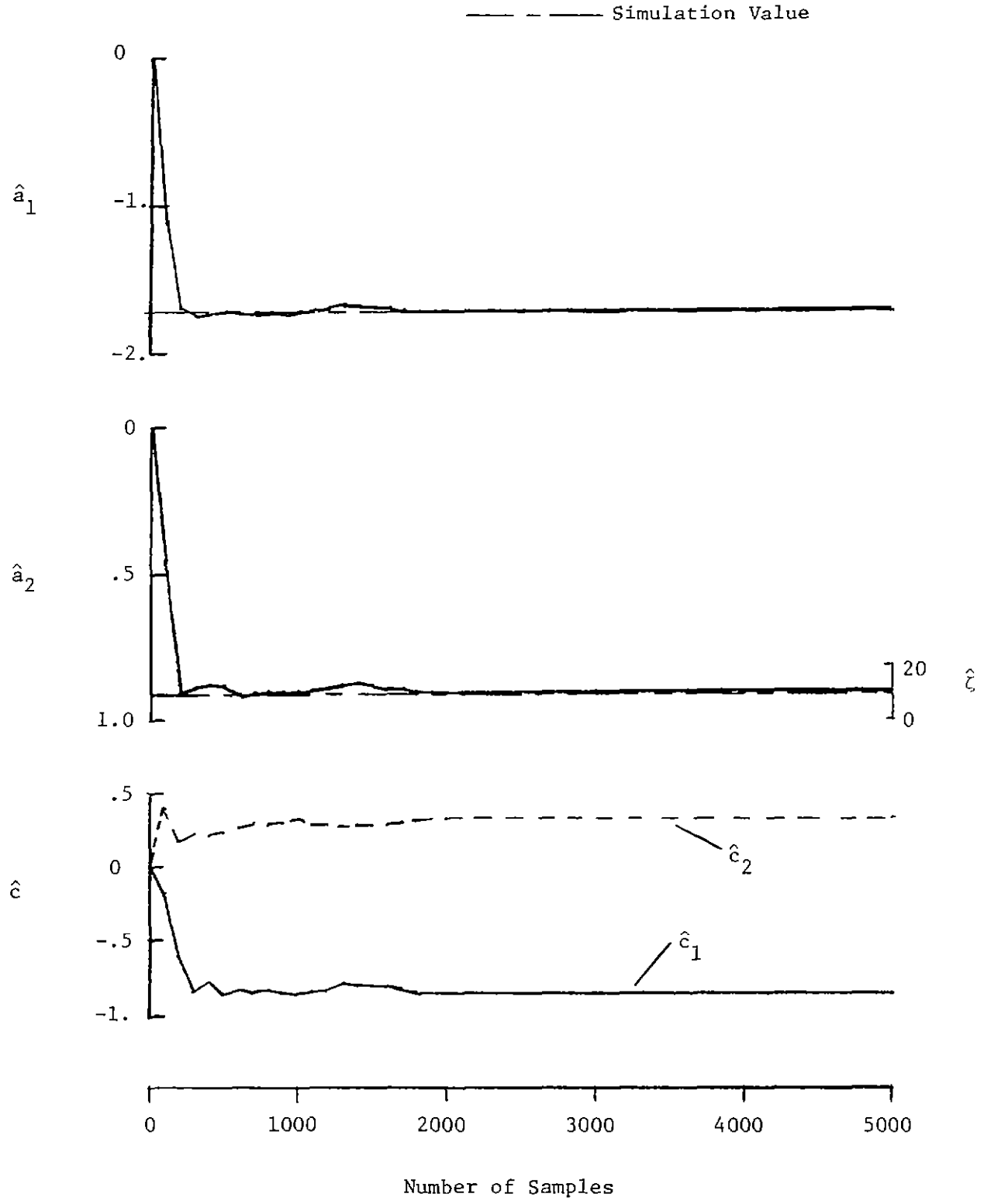

Figure 5. - Identified Parameter Convergence with Initial Parameter Estimates Set to Zero (RMS of Random Response = .25 deg, σ_r=.1 deg, σ_w=.2 deg/sec^2, Δt=.02 sec, ω_n=23.15 rad/sec, ζ=10%).

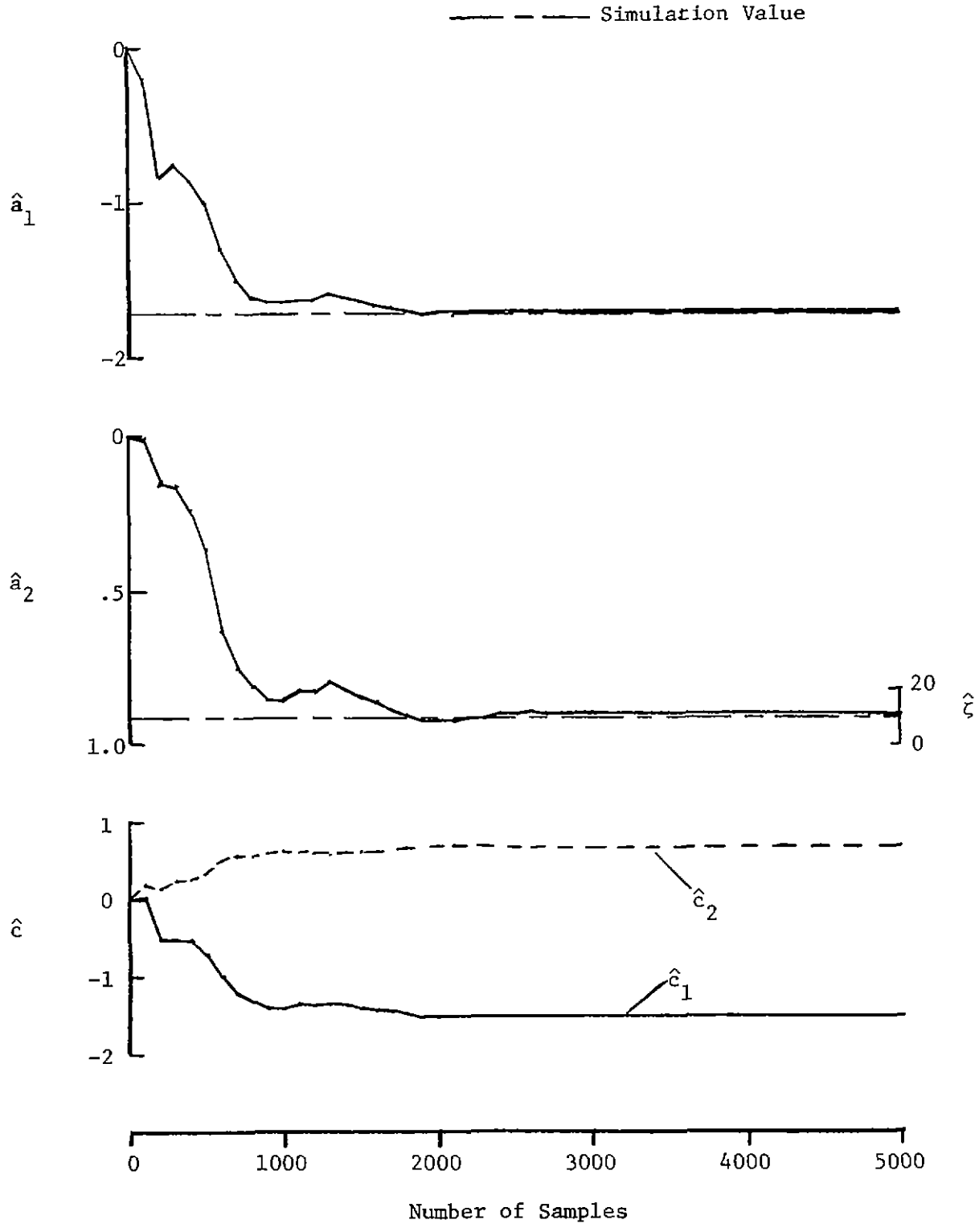

Figure 6. - Identified Parameter Convergence with Initial Parameter Estimates Set to Zero (RMS of Random Response = .05 deg, σ_r=.1 deg, σ_w=.04 deg/sec^2, Δt=.02 sec, ω_n=23.15 rad/sec, ζ=10%).

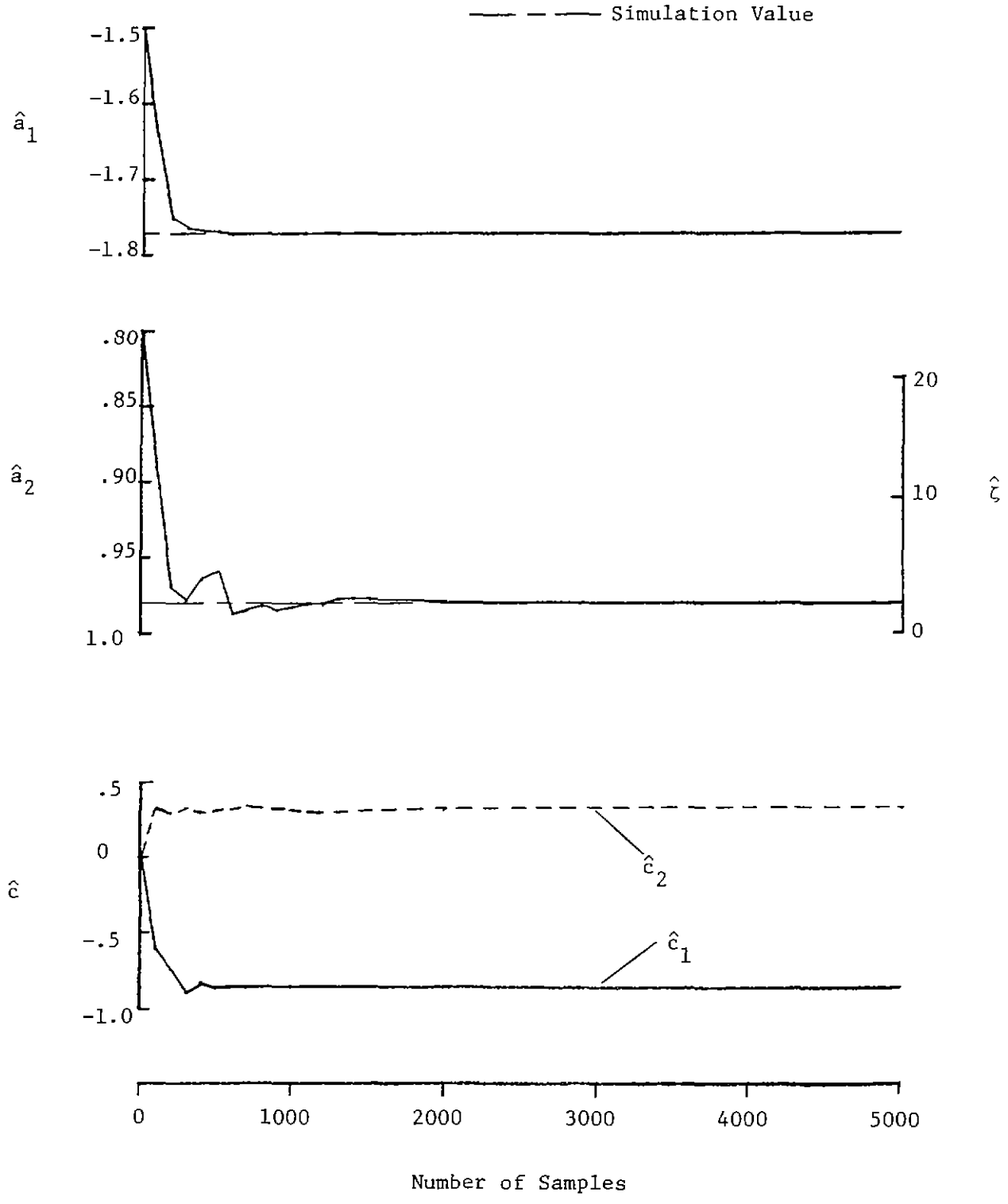

Figure 7. - Identified Parameter Convergence (RMS of Random Response = .75 deg, σ_r=.1 deg, σ_w=.2 deg/sec^2, Δt=.02 sec, ω_n=23.15 rad/sec, ζ=2%).

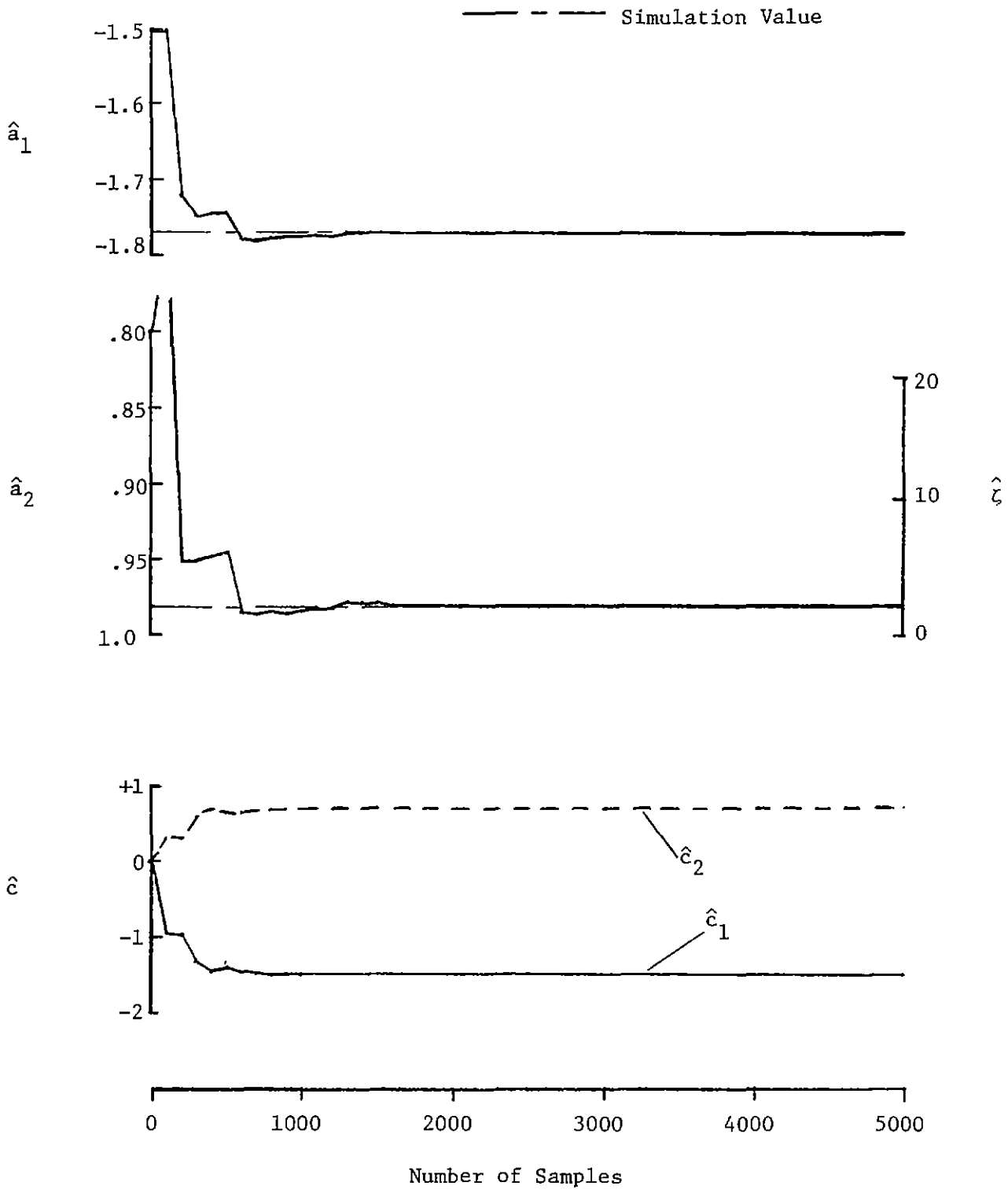

Figure 8. - Identified Parameter Convergence (RMS of Random Response = .15 deg, σ_r=.1 deg, σ_w=.04 deg/sec^2, Δt=.02 sec, ω_n=23.15 rad/sec, ζ=2%).

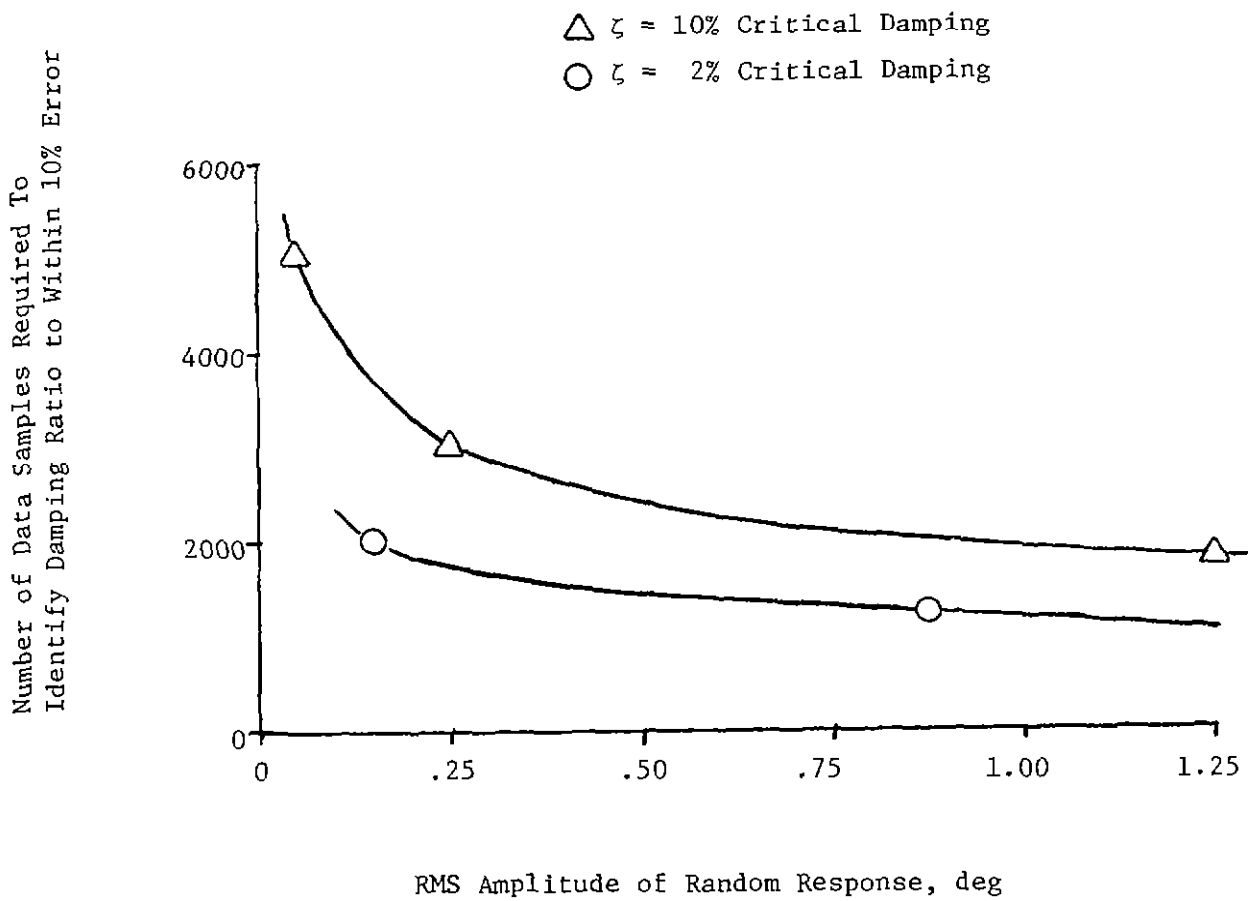

Figure 9. - Number of Data Samples Required To Identify Damping Ratio to Within 10% Error vs. RMS Amplitude of Random Response (Simulation Results, σ_r=.1 deg, Δt=.02 sec, ω_n=23.15 rad/sec).

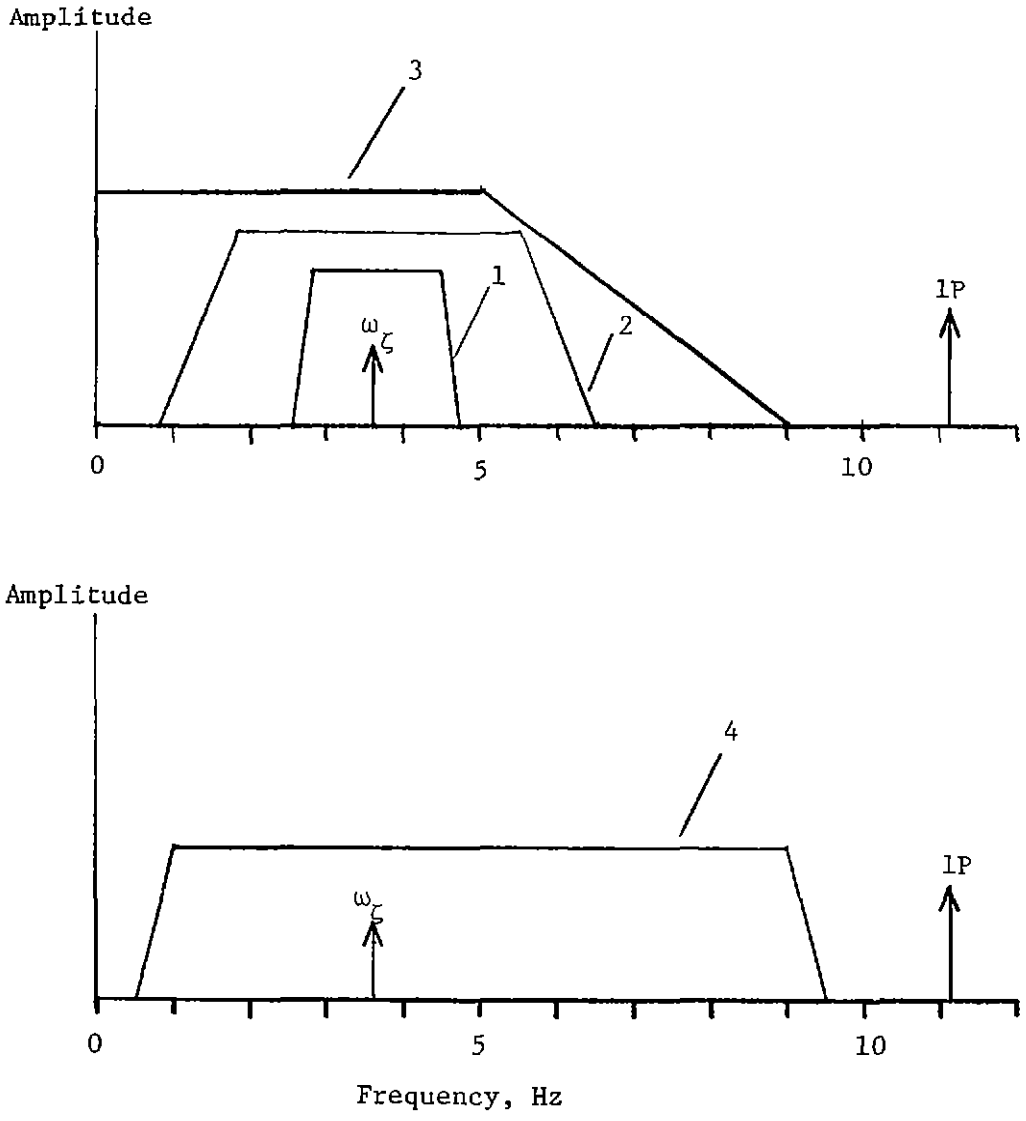

Figure 10. - Amplitude vs. Frequency Characteristics of Digital Filters Used to Separate the Desired Mode (1p = 11.17 Hz, ω_ζ=23.15 rad/sec (3.68 Hz)).

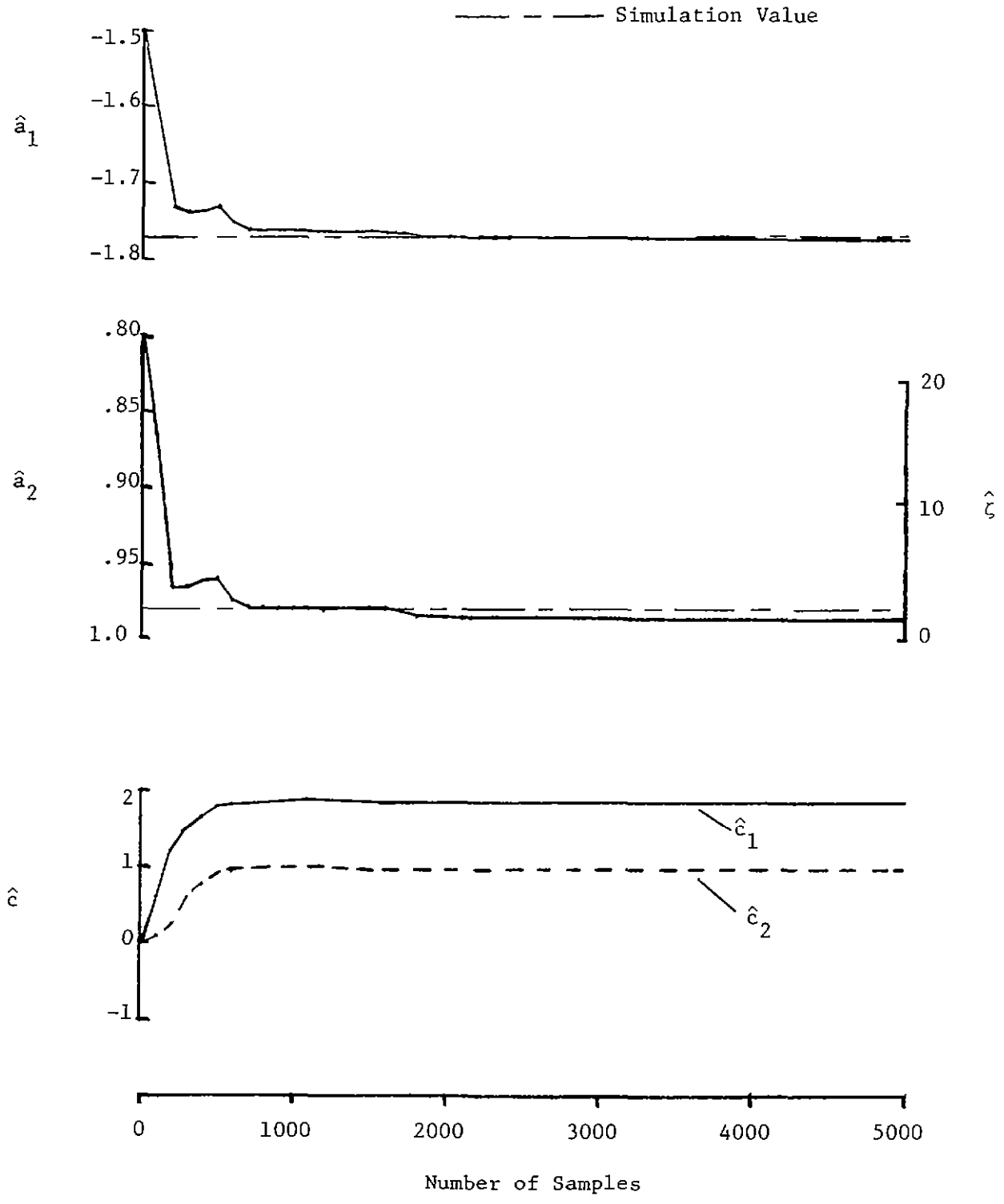

Figure 11. - Identified Parameter Convergence Using Digital Filter Number 4 (RMS of Random Response = .75 deg, σ_r=.1 deg, σ_w=.2 deg/sec^2, Δt=.02 sec, ω_n=23.15 rad/sec, ζ=2%).

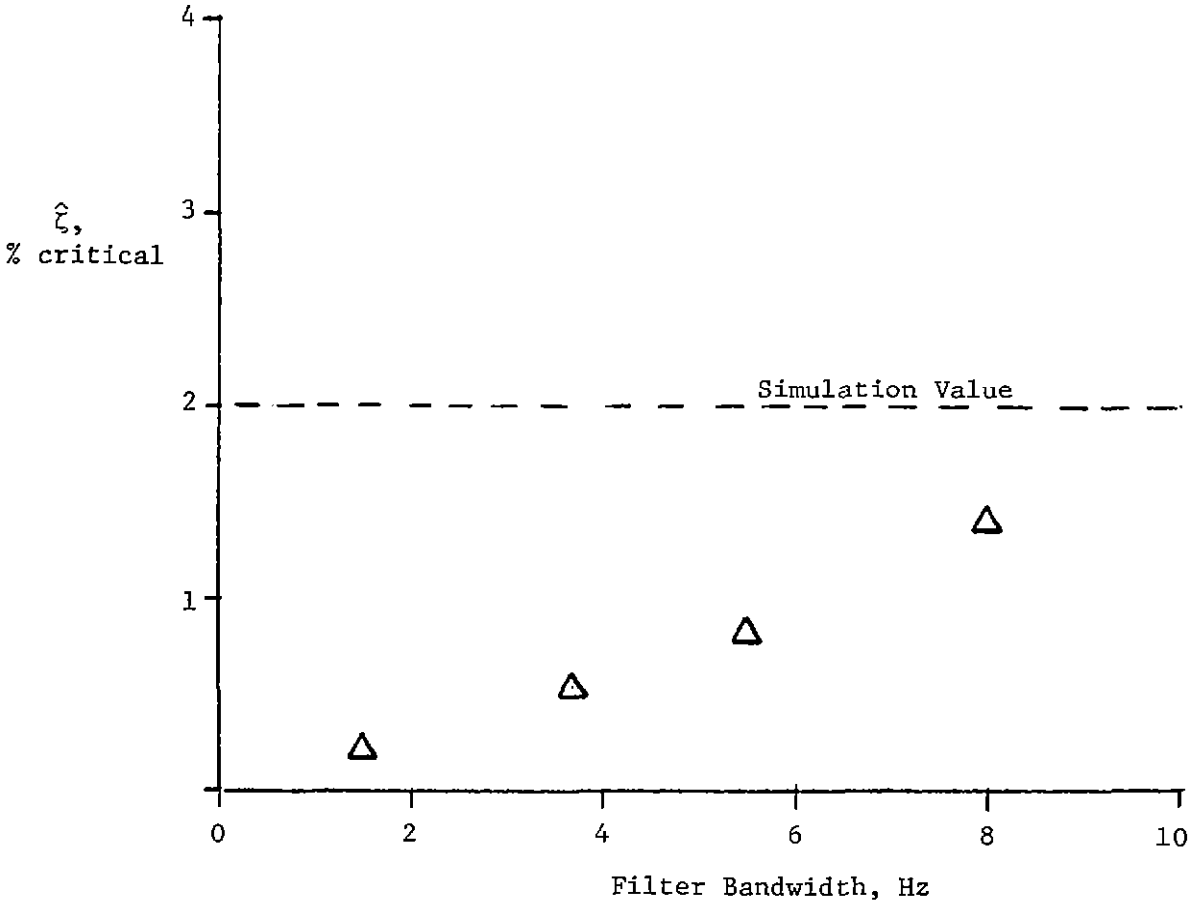

Figure 12. - Effect of Filter Bandwidth on Identified Damping Ratio (RMS of Random Response = .75 deg, σ_r=.1 deg, σ_w=.2 deg/sec^2, Δt=.02 sec, ω_n=23.15 rad/sec, ζ=2%).

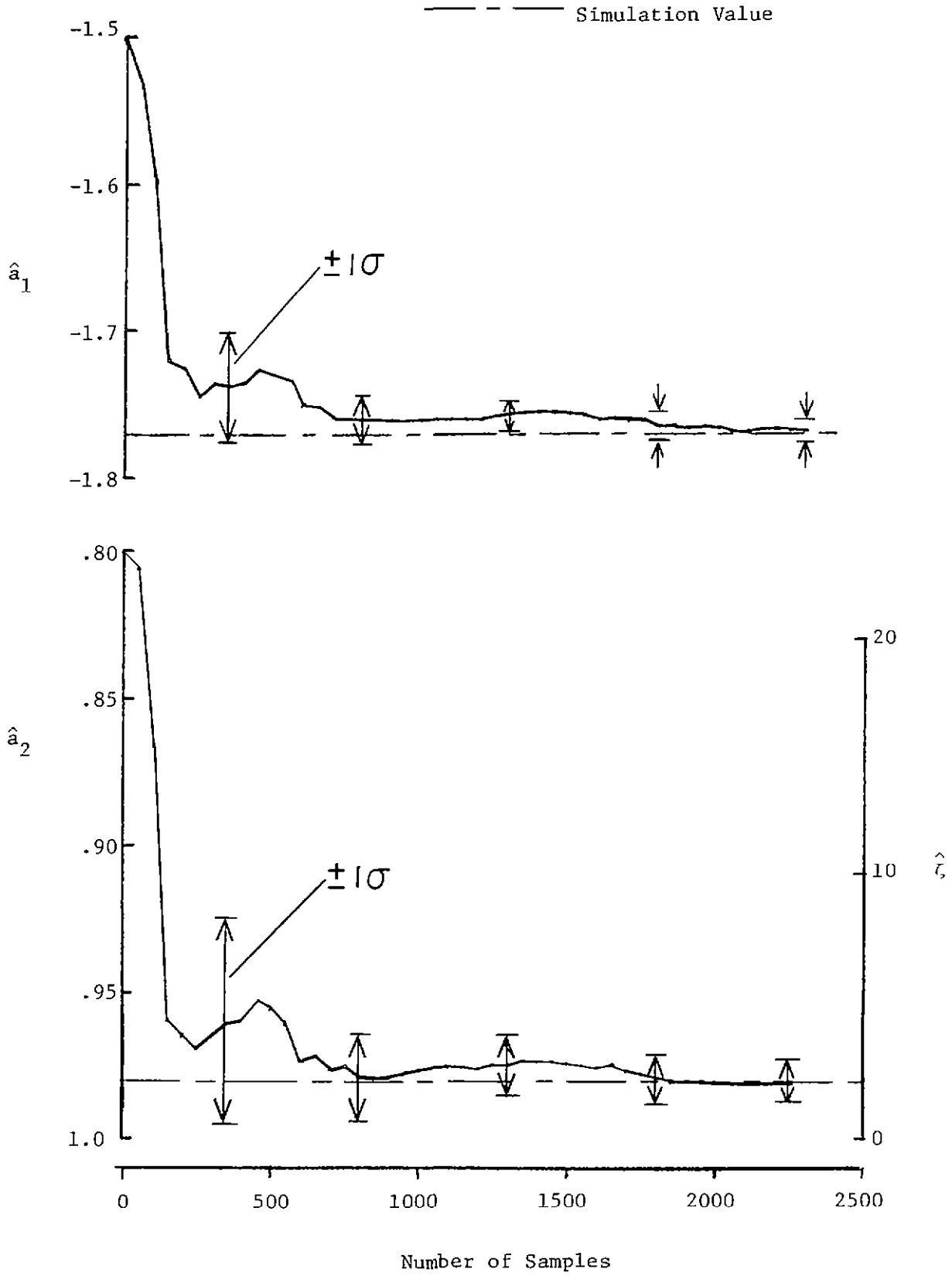

Figure 13. - Identified Parameter Convergence Showing the Computed Standard Deviation of the Estimate (RMS of Random Response = .75 deg, Filter Number 4, σ_r=.1 deg, σ_w=.2 deg/sec^2, ω_n=23.15 rad/sec).

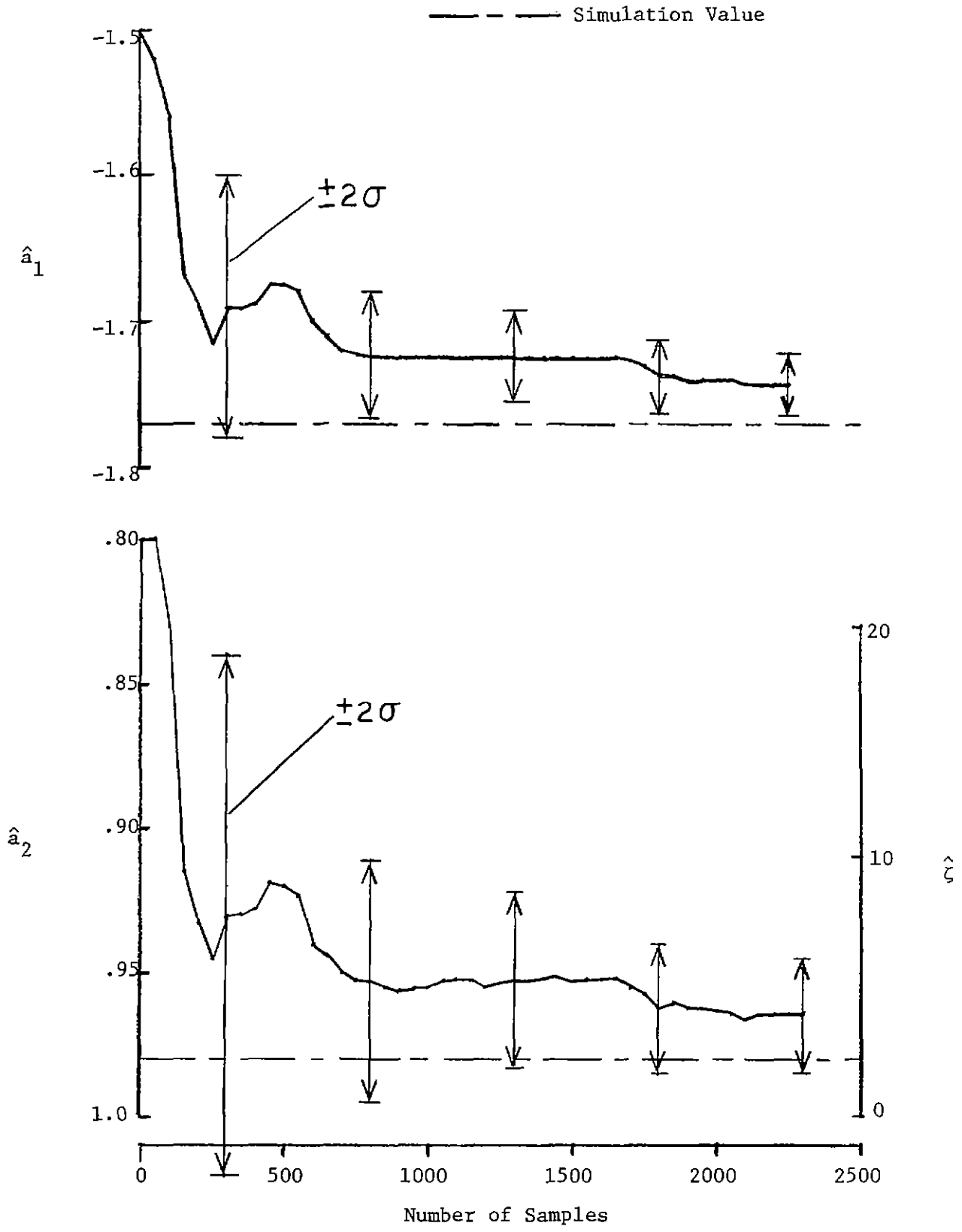

Figure 14. - Identified Parameter Convergence Showing the Computed 2 - Standard Deviation Band (RMS of Random Response = .37 deg, Filter Number 4, σ_r=.1 deg, σ_w=.04 deg/sec^2, ω_n=23.15 rad/sec).

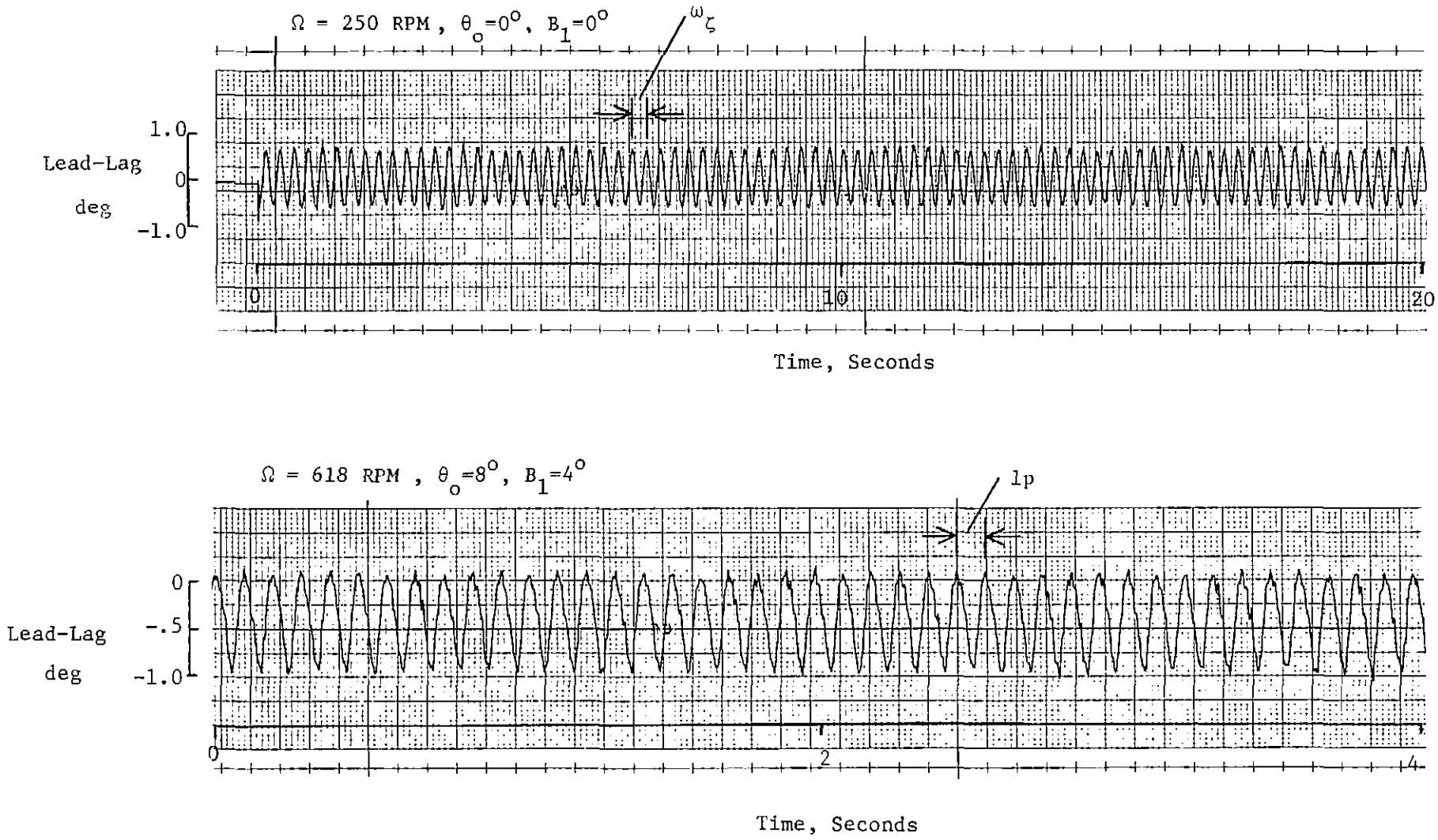

Figure 15. – Hover Facility Test Data Used to Identify Damping and Frequency of the Inplane Mode at Ω = 250 and Ω = 618 RPM. (Only a Portion of the Data is shown, Amplitude Scale is Approximate)

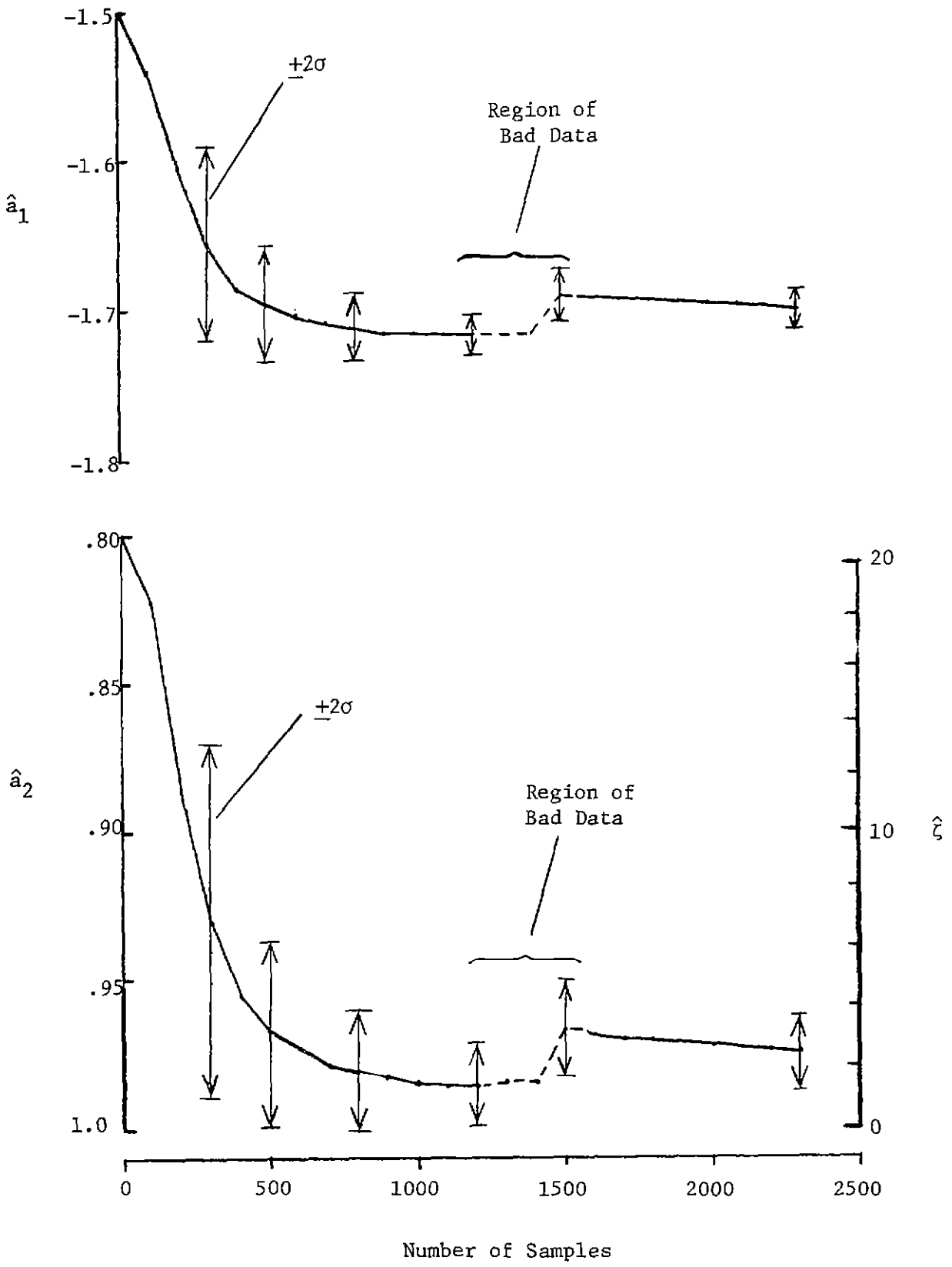

Figure 16. - Identified Parameter Convergence From Hover Facility Test Data at Ω = 250 RPM (Parameter Accuracy is Best before Region of Bad Data is encountered at 1200 samples, Δt=.02 sec).

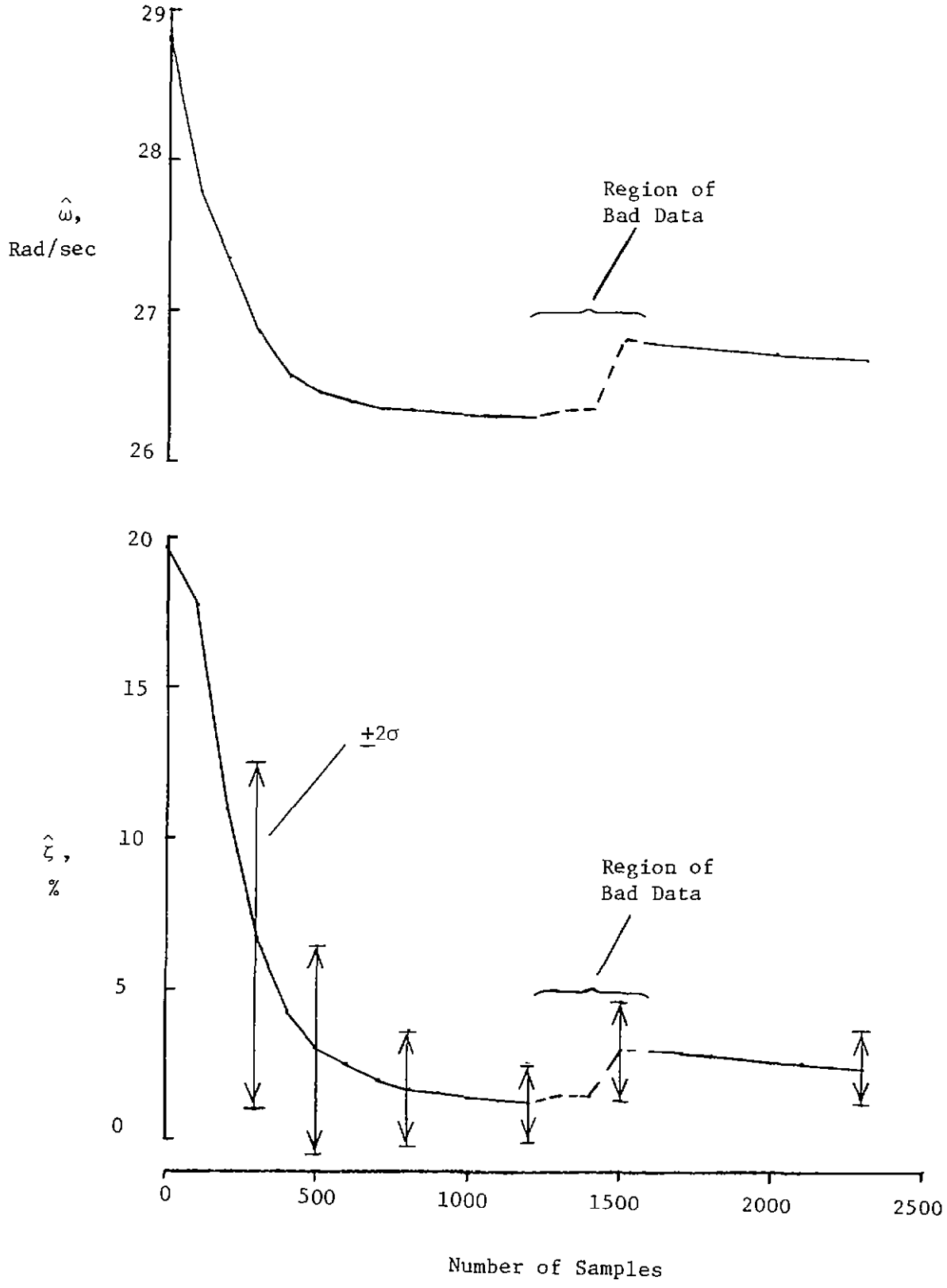

Figure 17. - Identified Damping and Frequency Parameter Convergence From Hover Facility Test Data at Ω = 250 RPM (Parameter Accuracy is Best before Region of Bad Data is encountered at 1200 samples, Δt=.02 sec).

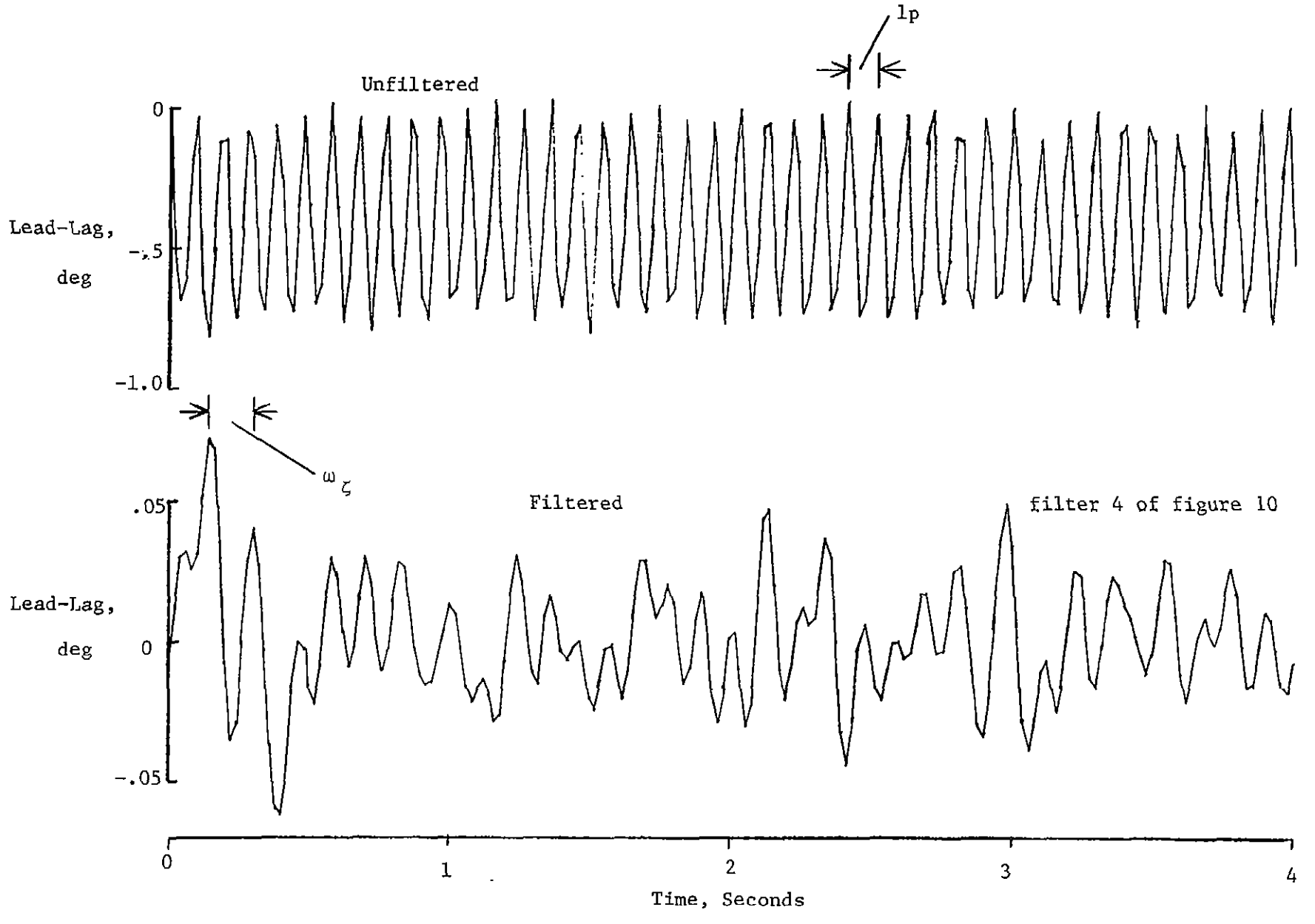

Figure 18. - Hover Facility Test Data at Ω = 618 RPM Showing Unfiltered and Filtered Test Data (Only a portion of Data is shown, Amplitude Scale is Approximate , Θ_o= 8°, B_1=4°)

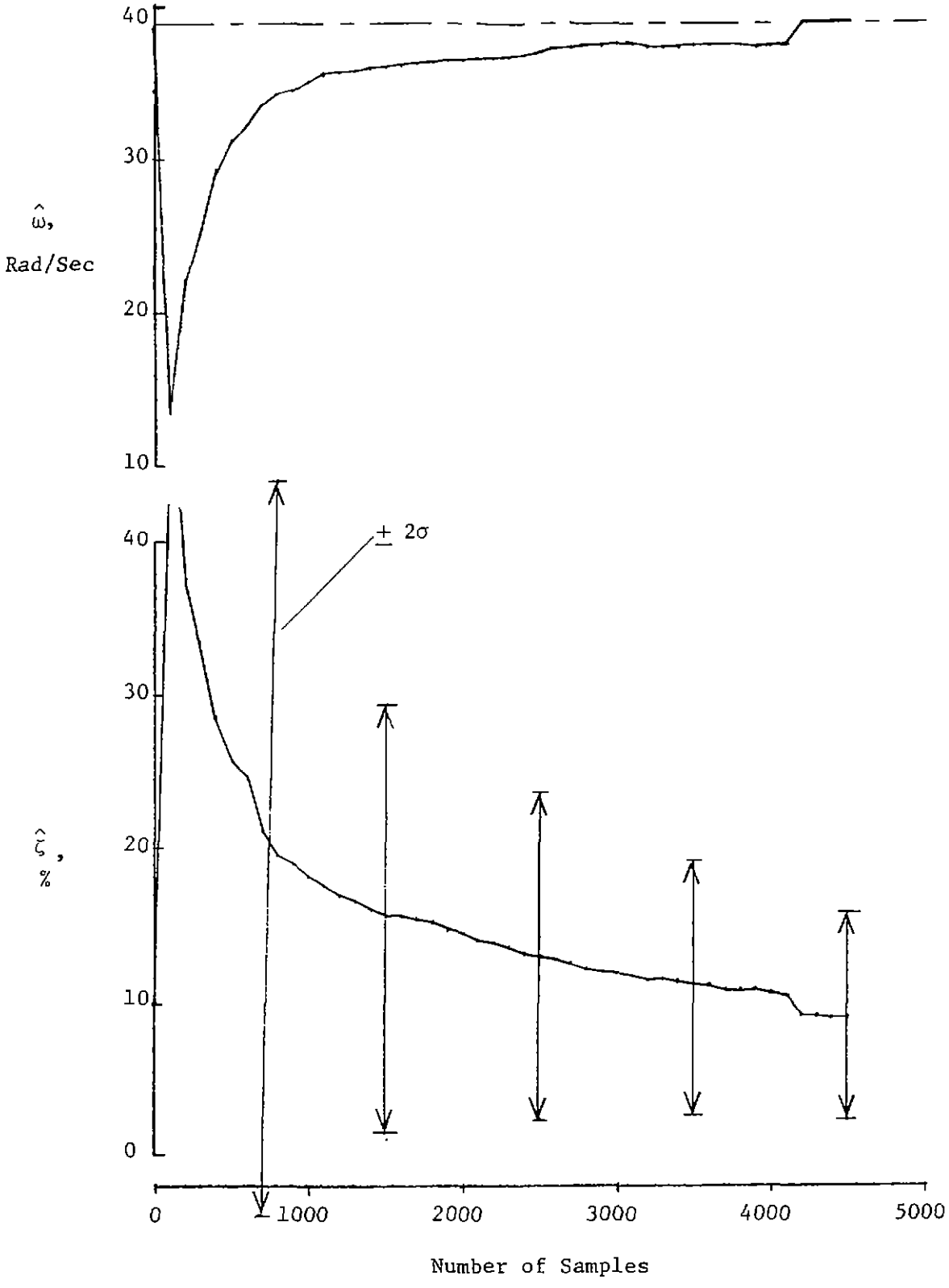

Figure 19. - Identified Damping and Frequency Parameter Convergence From Hover Facility Test Data at Ω=618 RPM (Δt=.01 sec, RMS of Random Response ≃ .03 deg, twice the available Data Length is needed to achieve desired damping accuracy).

1. Report No.	2. Government Accession No.	3. Recipient's Catalog No.
NASA CR-3600		

4. Title and Subtitle	5. Report Date
ROTORCRAFT BLADE MODE DAMPING IDENTIFICATION FROM RANDOM RESPONSES USING A RECURSIVE MAXIMUM LIKELIHOOD ALGORITHM	September 1982
	6. Performing Organization Code
7. Author(s)	8. Performing Organization Report No.
John A. Molusis	
	10. Work Unit No.
9. Performing Organization Name and Address John A. Molusis Applied Research Consultant Varga Road, P. O. Box 81 Ashford, CT 06278	11. Contract or Grant No.
	13. Type of Report and Period Covered Contractor Report
12. Sponsoring Agency Name and Address National Aeronautics and Space Administration Washington, DC 20546	14. Sponsoring Agency Code 505-42-13-04 (L-26971B)

15. Supplementary Notes

The contract research was financially supported by the Structures Laboratory, U.S. Army Research and Technology Laboratories (AVRADCOM). Langley Technical Monitor: Warren H. Young, Jr.
Final Report

16. Abstract

An on-line technique is presented for the identification of rotor blade modal damping and frequency from rotorcraft random response test data. The identification technique is based upon a recursive maximum likelihood (RML) algorithm, which is demonstrated to have excellent convergence characteristics in the presence of random measurement noise and random excitation. The RML technique requires virtually no user interaction, provides accurate confidence bands on the parameter estimates, and can be used for continuous monitoring of modal damping during wind tunnel or flight testing.

Results are presented from simulation random response data which quantify the identified parameter convergence behavior for various levels of random excitation. The data length required for acceptable parameter accuracy is shown to depend upon the amplitude of random response and the modal damping level. Random response amplitudes of 1.25 degrees to .05 degrees are investigated. The RML technique is applied to hingeless rotor test data from the NASA Langley Research Center Helicopter Hover Facility. The inplane lag regressing mode is identified at different rotor speeds. The identification from the test data is compared with the simulation results and with other available estimates of frequency and damping.

17. Key Words (Suggested by Author(s))	18. Distribution Statement
Helicopter Rotors Rotor Blade Modes Parameter Identification Recursive Maximum Likelihood Random Response Data	Unclassified - Unlimited Subject Category 05

19. Security Classif. (of this report)	20. Security Classif. (of this page)	21. No. of Pages	22. Price
Unclassified	Unclassified	48	A03

For sale by the National Technical Information Service, Springfield, Virginia 22161